Molecular Pharmacology Fast Forward. Published on June 24, 2004 as doi:10.1124/mol.104.000760
This article has not been copyedited and formatted. The final version may differ from this version.

Evidence for a novel K^+ channel modulated by α_{1A}-adrenoceptors in cardiac myocytes.

By

Stéphanie CM Choisy, Jules C Hancox, Lesley A Arberry,

A Martyn Reynolds, Michael J Shattock & Andrew F James.

Department of Physiology and Cardiovascular Research Laboratories, School of Medical Sciences, University of Bristol, Bristol, United Kingdom (SCMC, JCH, LAA, AFJ).

Department of Renal Medicine, GKST, King's College School of Medicine & Dentistry, London, United Kingdom (AMR).

Cardiac Physiology, Centre for Cardiovascular Biology & Medicine, GKST, St Thomas' Hospital, London, United Kingdom (MJS).

Molecular Pharmacology Fast Forward. Published on June 24, 2004 as DOI: 10.1124/mol.104.000760
This article has not been copyedited and formatted. The final version may differ from this version.

RUNNING TITLE:

A novel phenylephrine-modulated cardiac K^+ channel

Corresponding author: Dr Andrew F James, Department of Physiology and Cardiovascular Research Laboratories, School of Medical Sciences, University of Bristol, University Walk, Bristol, BS8 1TD, United Kingdom.
Tel: +44-117-928-9187; Fax: +44-117-928-8923; e-mail: a.james@bristol.ac.uk

Text pages: 35.
Tables: 1.
Figures: 12.
References: 40.
Abstract: 248 words.
Introduction: 698 words.
Discussion: 1497 words.

ABBREVIATIONS: α_1-AR, α_1-adrenoceptor; A61603, an α_{1A}-adrenoceptor-selective agonist; GDPβS, guanosine 5'-[β-thio]diphosphate; I_t, the transient (inactivating) current; I_{ss}, the steady-state outward current; $I_{ss,PE}$, the phenylephrine-sensitive component of I_{ss}; K_{2P}, two pore domain K^+ channel; K_v, voltage-gated K^+ channel; PE, phenylephrine; PI 3-kinase, phosphatidylinositol 3-kinase; PTX, pertussis toxin; Slick, Sequence Like an Intermediate Conductance K^+ channel; TASK, two pore domain acid-sensitive K^+ channel; TEA, tetraethylammonium, TREK, two pore domain related K^+ channel; WB4101, an α_{1A}-adrenoceptor-selective antagonist

Molecular Pharmacology Fast Forward. Published on June 24, 2004 as DOI: 10.1124/mol.104.000760
This article has not been copyedited and formatted. The final version may differ from this version.

ABSTRACT

Accumulating evidence suggests that steady-state K^+ currents modulate excitability and action potential duration, particularly in cardiac cell types with relatively abbreviated action potential plateau phases. Despite representing potential drug targets, at present these currents and their modulation are comparatively poorly characterized. Therefore, we investigated the effects of phenylephrine (PE; an α_1-adrenoceptor, α_1-AR, agonist) on a sustained outward K^+ current in rat ventricular myocytes. Under K^+ current-selective conditions at 35°C and whole-cell patch clamp, membrane depolarization elicited transient (I_t) and steady-state (I_{ss}) outward current components. PE (10μM) significantly decreased I_{ss} amplitude, without significant effect on I_t. Preferential modulation of I_{ss} by PE was confirmed by intracellular application of the voltage-gated K^+ channel blocker tetraethylammonium, which largely inhibited I_t without affecting the PE-sensitive current ($I_{ss,PE}$). $I_{ss,PE}$ had the properties of an outwardly rectifying steady-state K^+-selective conductance. Acidification of the external solution or externally applied $BaCl_2$ or quinidine strongly inhibited $I_{ss,PE}$. However, $I_{ss,PE}$ was not abolished by the inhibitors of TASK acid-sensitive background K^+ channels, anandamide, ruthenium red and zinc. Furthermore, the PE-sensitive current was partially inhibited by external administration of high concentrations of the voltage-gated K^+ channel blockers, tetraethylammonium and 4-aminopyridine. Power spectrum analysis of $I_{ss,PE}$ yielded a large unitary conductance of 78pS. $I_{ss,PE}$ resulted from PE activation of the α_{1A}-AR sub-type, involved a pertussis toxin-insensitive G-protein and was independent of cytosolic Ca^{2+}. Collectively, these results demonstrate that α_{1A}-AR activation results in the inhibition of an outwardly rectifying steady-state K^+ current with properties distinct from previously characterized cardiac K^+ channels.

Molecular Pharmacology Fast Forward. Published on June 24, 2004 as DOI: 10.1124/mol.104.000760
This article has not been copyedited and formatted. The final version may differ from this version.

The exceptional diversity of K^+ channels has particular significance in the heart, where different currents contribute to distinct phases of the cardiac action potential (Snyders, 1999). Steady-state, or plateau, currents show very rapid activation and relatively slow or no inactivation and thereby contribute outward current through out phases 1 and 2, and for the early part of phase 3 of the action potential. They are therefore thought to be of particular importance in cardiac cell types with relatively abbreviated plateau phases (Nattel et al., 1999, Snyders, 1999). However, in comparison with the transient outward (I_{to1}) and delayed rectifier (I_K) K^+ currents, little is known about the steady-state currents and their modulation (Nattel et al., 1999, Snyders, 1999).

The steady-state currents represent a diverse family that include the so-called ultra-rapid delayed rectifiers (I_{Kur}) of mouse ventricular myocytes and human and canine atrial myocytes (Nattel et al., 1999). Although themselves molecularly diverse, being comprised of Kv1.2, Kv1.5, Kv2.1 or Kv3.1 voltage-gated K^+ channel α-subunits, I_{Kur} are distinguished from other steady-state currents by their sensitivity to the K^+ channel blocker, 4-aminopyridine (4-AP; IC_{50} 5-50μM) (Nattel et al., 1999). Other, less well-characterized, steady-state currents include I_{Kp} of guinea-pig ventricular myocytes and I_{ss} of rat atrial and ventricular myocytes (Apkon and Nerbonne, 1991, Backx and Marban, 1993, Himmel et al., 1999, van Wagoner et al., 1996). Rat I_{ss} is at least an order of magnitude less sensitive to 4-AP than is I_{Kur} (Apkon and Nerbonne, 1991, Himmel et al., 1999). Rat I_{ss} is also only partially inhibited by external application of tetraethylammonium (TEA), another voltage-gated K^+ channel blocker (Himmel et al., 1999, Snyders, 1999).

Slick (Sequence Like an Intermediate Conductance K^+ channel, or slo 2.1) is a rapidly activating large conductance voltage-gated K^+ channel that has recently been shown to be selectively expressed in the brain and the heart (Bhattacharjee et al., 2003). To date no endogenous currents for Slick have been identified. However, in principle, since it produces

Molecular Pharmacology Fast Forward. Published on June 24, 2004 as DOI: 10.1124/mol.104.000760
This article has not been copyedited and formatted. The final version may differ from this version.

relatively sustained outward currents that are partially sensitive to external TEA, Slick could contribute to cardiac steady-state K^+ currents (Bhattacharjee et al., 2003). Similarly, the recently identified two-pore domain K^+ channels (K_{2P}) channels that form almost instantaneous, non-inactivating background outward currents could also contribute to cardiac steady-state currents (Lesage and Lazdunski, 2000). mRNA and protein for TASK-1, an acid-sensitive K_{2P} channel thought to play a role in the modulation of membrane excitability by G-protein-coupled receptor stimulation in neuronal cells (Millar et al., 2000, Talley et al., 2000), have been isolated from the heart (Barbuti et al., 2002, Duprat et al., 1997, Jones et al., 2002, Kim et al., 1999, Leonoudakis et al., 1998). Therefore, it has been suggested that TASK-1 channels contribute to the modulation of cardiac excitability and refractoriness (Barbuti et al., 2002, Duprat et al., 1997, Jones et al., 2002, Kim et al., 1999, Leonoudakis et al., 1998). Furthermore, TREK-1, an outwardly rectifying mechano-sensitive K_{2P} channel activated by membrane stretch or polyunsaturated fatty acids, is thought to underlie a G-protein-coupled receptor-modulated arachidonic acid-sensitive current, $I_{K.AA}$, in rat cardiac myocytes (Aimond et al., 2000, Patel et al., 1998, Terrenoire et al., 2001).

Many cardiac K^+ currents, including the inward rectifier (I_{K1}), transient outward current (I_{to1}) and ultrarapidly activating outward rectifier (I_{Kur}) currents are modulated by α_1-adrenoceptor (α_1-AR) stimulation (Fedida et al., 1993a, Nattel et al., 1999). In addition, there is evidence that the α_1-AR agonist, phenylephrine (PE), inhibits a relatively sustained outward current in rat cardiac myocytes (Ertl et al., 1991, Ravens et al., 1989, van Wagoner et al., 1996). Although the properties of this current are unclear, it has previously been suggested to represent a subtype of the voltage-gated K^+ current, I_{Kur} (Nattel et al., 1999, van Wagoner et al., 1996). Three subtypes of α_1-AR, α_{1A}, α_{1B} and α_{1D}, are expressed in the rat ventricle (Homma et al., 2000) and different receptor subtypes coupling with separate signaling pathways have been shown to modulate distinct canine ventricular K^+ currents

Molecular Pharmacology Fast Forward. Published on June 24, 2004 as DOI: 10.1124/mol.104.000760
This article has not been copyedited and formatted. The final version may differ from this version.

(Wang et al., 2001). The objectives of this study, therefore, were: (1) to examine the properties of PE-sensitive K^+ currents of rat ventricular myocytes, with particular emphasis on steady-state current, and (2) to establish the receptor signaling pathways mediating the predominant effects of α_1-AR stimulation.

Molecular Pharmacology Fast Forward. Published on June 24, 2004 as DOI: 10.1124/mol.104.000760
This article has not been copyedited and formatted. The final version may differ from this version.

METHODS

Drugs and Reagents

Anandamide, chelerythrine, genistein, bisindolylmaleimide I (GF109203X), methylarachidonyl fluorophosfonate (MAFP), neomycin sulphate, pertussis toxin, PKCε inhibitor peptide, staurosporine, 1-[6-((17β-3-methoxyestra-1,3,5(10)-trien-17-yl)amino)hexyl]-1H-pyrrole-2,5-dione (U73122), 1-[6-((17β-3-methoxyestra-1,3,5(10)-trien-17-yl)amino)hexyl]-1H-2,5-pyrrolidinedione (U73343), wortmannin were purchased from Calbiochem (Nottingham, UK), arachidonyl tri-fluoromethylketone ($AACOCF_3$) and the G_q-protein antagonist peptide GP2A were from Biomol (Exeter, UK) and A61603 and WB4101 were from Tocris (Bristol, UK). All other reagents were purchased from Sigma (Poole, UK).

A61603, atenolol, carbachol, chloroethylclonidine (CEC), isoprenaline, neomycin sulfate, pertussis toxin, phenylephrine (PE) and WB4101 were dissolved at 1000-times final concentration in de-ionized water (dH_2O) immediately prior to use. In this study, 10μM PE was used as a maximally effective concentration of the α_1-AR agonist (Fedida et al., 1993a). The PKCε inhibitor and the GP2A G_q-protein antagonist peptides were dissolved in dH_2O and stored at –20^{o}C until use. Nifedipine and prazosin were stored at 4^{o}C as stock solutions of at least 1000-times final concentration in ethanol. To avoid oxidation during storage, $AACOCF_3$, anandamide, MAFP, U73122 and U73343 were aliquoted to the appropriate amounts for experimental use by solution in chloroform under a nitrogen atmosphere and all chloroform evaporated prior to storage at –20^{o}C. Prior to addition to experimental solutions, these reagents were dissolved in ethanol or dimethyl sulfoxide (DMSO) to at least 1000-times final concentration. External experimental solutions containing 4-aminopyridine (4-AP), tetraethylammonium chloride (TEA) and quinidine were made up at the final concentration immediately prior to use. The 50mM TEA solution was made by equimolar replacement of

Molecular Pharmacology Fast Forward. Published on June 24, 2004 as DOI: 10.1124/mol.104.000760
This article has not been copyedited and formatted. The final version may differ from this version.

NaCl with TEA. All other reagents were dissolved in DMSO at least 1000-times the final concentration, aliquoted and stored at –20^{o}C until use.

Myocyte isolation

Male Wistar rats (200-250g) were killed humanely according to UK government legislation. The heart was excised rapidly and mounted on a Langendorff apparatus and retrogradely perfused via the aorta with a series of solutions, at 37^{o}C, based on an isolation solution comprising (in mM): 130 NaCl, 5.4 KCl, 1.4 $MgCl_2$, 0.4 NaH_2PO_4, 4.2 HEPES, 10 D-glucose, 20 taurine, 10 creatine, pH 7.3. Hearts were initially perfused for 2-4 min with a solution containing 750μM $CaCl_2$. The heart was then perfused for 4 min with a Ca^{2+}-free isolation solution containing 100μM EGTA and this was followed by perfusion with isolation solution containing 1mg ml^{-1} Worthington type 2 collagenase (Lorne Laboratories, Reading, UK), 0.1mg ml^{-1} protease (Sigma, Type XIV) and 0.1% dialyzed bovine serum albumin (Sigma A-6003). After 8 min, the heart was removed from the apparatus and the left ventricular free wall finely chopped and gently agitated in fresh enzyme-containing solution at 37^{o}C. The tissue was agitated for 4 min periods, after which the tissue was filtered through nylon gauze to separate dissociated cells from the remaining undigested tissue. The undigested tissue was then further treated with fresh enzyme solution. Dissociated cells were sedimented by centrifugation and re-suspended in Ca^{2+}-free isolation solution. The cells were then re-sedimented and re-suspended 3-times, at each re-suspension incrementing the Ca^{2+} to a final concentration of 750μM. Cells were stored in this Ca^{2+}-containing isolation solution at room temperature and used within 9 hours of isolation.

Whole cell recording

Cells were superfused with an external solution comprising (in mM): 134 NaCl, 4 KCl, 1.2 $MgCl_2$, 1 $CaCl_2$, 10 HEPES, 11 D-glucose, pH 7.35 at 35^{o}C. Nifedipine (3μM) and

Molecular Pharmacology Fast Forward. Published on June 24, 2004 as DOI: 10.1124/mol.104.000760
This article has not been copyedited and formatted. The final version may differ from this version.

atenolol (1μM) were added to block L-type Ca^{2+} currents and β-adrenoceptors, respectively. K^+-free external solution was produced by equimolar replacement of KCl with CsCl. Pipettes were pulled from borosilicate glass capillaries (Corning #8250, A-M Systems, USA) to tip resistances of 1.5 – 3.0MΩ. Perforated patch recordings were made using a pipette solution comprising (in mM): 125 HCH_3O_3S, 125 KOH, 10 KCl, 5 NaCl, 5 $MgCl_2$, 10 HEPES, pH 7.2 (KOH) to which 225μg ml^{-1} amphotericin B was added according to a recipe kindly provided by Dr Andy Trafford (Manchester, UK). Conventional whole cell recordings were made using a pipette solution containing (in mM): 130 HCH_3O_3S, 130 KOH, 10 KCl, 10 EGTA, 2 $MgCl_2$, 1 $CaCl_2$, 10 HEPES, 4 MgATP, 0.2 Na_2GTP, pH 7.2 (KOH). The free Ca^{2+} concentration of this solution was calculated to be ~25nM using WCaBuf software kindly provided by Dr Guy Droogmans (Leuven, Belgium). For the majority of experiments, a low concentration of Na^+ was used in order to minimize the contribution of Na^+-dependent electrogenic transporters (*i.e.* Na^+/K^+ ATPase and Na^+/Ca^{2+} exchange) to the outward currents. In one series of experiments, a K^+-rich pipette solution containing 20 mM Na^+ was produced by equimolar replacement of KOH with NaOH. K^+-free pipette solutions were produced by equimolar replacement of KOH and KCl in the above recipe with Cs^+ or Li^+ salts. A K^+-rich pipette solution containing the voltage-gated K^+ channel blocker, tetraethylammonium (TEA; 20 mM) was produced by equimolar replacement of KOH with TEAOH. In some experiments, a virtually Ca^{2+}-free pipette solution was used in which EGTA was replaced with equimolar BAPTA and no $CaCl_2$ was added. In other experiments, GTP in the pipette solution was replaced with 1mM GDPβS. In our experience, removal of ATP from the pipette solution often leads to the activation of the ATP-sensitive K^+ channel current, $I_{K.ATP}$. Since $I_{K.ATP}$ is large (>30pA/pF), activation of this current may mask the effects of PE on other currents. Thus, it was not possible to test the sensitivity of the PE-sensitive current to intracellular ATP. Experiments on the L-type Ca^{2+} current ($I_{Ca,L}$) were

Molecular Pharmacology Fast Forward. Published on June 24, 2004 as DOI: 10.1124/mol.104.000760
This article has not been copyedited and formatted. The final version may differ from this version.

carried out using the Cs^+-rich pipette solution and by omitting nifedipine and atenolol from the superfusate.

Whole cell currents recorded by EPC-9 (HEKA GmbH, Germany) or Axopatch 200B (Axon Instruments Inc., USA) patch clamp amplifiers were recorded to the hard-disk of a PC using Pulse software (Vs 8.11, HEKA GmbH, Germany). While the EPC-9 amplifier had a built in A/D converter, currents recorded using the Axopatch 200B were acquired using an ITC-16 A/D converter (Instrutech Inc, USA). The sampling rate was typically 2kHz. Junction potentials and capacitance transients were compensated electronically. Currents were normalized to capacitance as a measure of cell size. Arrows in figures presenting current traces indicate the zero current level.

Analysis of current inactivation

The effect on peak and late outward currents of varying conditioning potential (CP) for 1s prior to depolarization to +40mV was examined. The dependence of the peak currents on CP from voltages of –80mV to +5mV (V_{CP}) were fitted with single or double Boltzmann equations, respectively, by non-linear least squares using IgorPro 3.16B software (Wavemetrics Inc, Lake Oswego, OR, USA) as follows:

$$I_{pk}(V_{CP}) = I_t/(1+\exp((V_{CP} - V_{0.5})/V_s)) + I_{ss} \quad (1)$$

$$I_{pk}(V_{CP}) = I_{to1}/(1+\exp((V_{CP} - V_{0.5,1})/V_{s,1})) + I_{Kx}/(1+\exp((V_{CP} - V_{0.5,2})/V_{s,2})) + I_{ss} \quad (2).$$

Where $V_{0.5}$ (likewise $V_{0.5,1}$ and $V_{0.5,2}$) represents the half-maximal voltage of inactivation, V_s (likewise $V_{s,1}$ and $V_{s,2}$) is the slope of the relation, I_t is the total inactivating current when data are fitted by a single Boltzmann, I_{to1} is the current inactivating at more negative potentials when the data are fitted by a double Boltzmann, I_{Kx} is the current inactivating at less negative potentials when the data are fitted by a double Boltzmann and I_{ss} is the non-inactivating

Molecular Pharmacology Fast Forward. Published on June 24, 2004 as DOI: 10.1124/mol.104.000760
This article has not been copyedited and formatted. The final version may differ from this version.

steady-state outward current (Himmel et al., 1999). Note the difference in the definition of I_t and I_{to1} between the two equations.

The time course of inactivation of outward currents were fitted with single or double exponential equations, respectively, by non-linear least squares using IgorPro 3.16B software as follows:

$$I(t) = A_0 + A_1.\exp(-t/\tau) \quad (3)$$

$$I(t) = A_0 + A_1.\exp(-t/\tau_1) + A_2.\exp(-t/\tau_2) \quad (4).$$

Where A_0 is the time-independent current, τ_1 and τ_2 are the rapid and slow time constants of inactivation and A_1 and A_2 are the maximal amplitudes of the rapidly and slowly inactivating currents, respectively. In some cases, the amplitude of the inactivating component of the outward currents was reported as the sum of the A_1 and A_2 components. Where the data were fitted by a single exponential component, A_2 was taken to be 0 and the reported value therefore represents the A_1 component alone.

Analysis of the concentration-dependence of 4-aminopyridine action

The effect of 4-aminopyridine on the time-independent A_0 component was expressed as a percentage reduction from control:

$$\%\text{reduction} = ((A_{0,\text{control}} - A_{0,4\text{-AP}})/A_{0,\text{control}}) \times 100, \quad (5)$$

where $A_{0,\text{control}}$ represents the control value and $A_{0,4\text{-AP}}$, the value of A_0 in the presence of 4-AP. The concentration dependence of 4-AP action was fitted by a logistic equation as follows:

$$\%\text{reduction} = \%\text{reduction}_{max}/(1 + (IC_{50}/[4\text{-AP}])^{nH}), \quad (6)$$

Molecular Pharmacology Fast Forward. Published on June 24, 2004 as DOI: 10.1124/mol.104.000760
This article has not been copyedited and formatted. The final version may differ from this version.

where %reduction$_{max}$ is the maximal percentage reduction, IC_{50} is the concentration at which the current was reduced by 50% of control and nH is the Hill coefficient.

Spectral analysis of current variance

The variance of the phenylephrine (PE)-sensitive currents was calculated from the integral of the spectral density function, as follows (Dempster, 1993, Helliwell and Large, 1998). Outward currents elicited by depolarization to +40mV were sampled at 2kHz and passed through an 8-pole Bessel filter with a cut-off frequency (f_B) of 1kHz. Under our recording conditions the whole cell configuration simulates a single-pole filter with a cut-off frequency of

$$f_{RC}=1/(2\pi R_s C_m) \quad (7)$$

where R_s = series resistance and C_m=membrane capacitance. Therefore, only data from cells with a membrane time constant ($\tau_m = R_s C_m$) < 720μs were included in the analysis (mean τ_m = 556 ± 41μs, *n*=8). The last 1024 data points (*i.e.* 512ms) of recorded currents were used for calculation of the power spectrum. The DC and inactivating components of the currents were subtracted by fitting a single decaying exponential equation to the time course of inactivation and subtracting the current predicted by the fitted equation from the data trace. A Hanning (cosine) window was applied to the data and the power spectrum calculated using the Fast Fourier Transform function of IgorPro 3.16B, with appropriate re-scaling (Dempster, 1993). Each current trace was analyzed in blocks of 256 data points and between 3 and 5 current traces were used to calculate an averaged spectrum. Thus, the lowest frequency that could be resolved was 7.8Hz (*i.e.* 2kHz/256) and the highest corresponded to the Nyquist frequency of 1kHz. However, since the cut-off frequency of the whole cell configuration, f_{RC}, for the eight cells included in the analysis ranged from 250Hz to 400Hz (297 ± 22 Hz, *n*=8), only data ranging from the 7.8Hz to 400Hz were included in the analysis (Helliwell and Large, 1998).

Molecular Pharmacology Fast Forward. Published on June 24, 2004 as DOI: 10.1124/mol.104.000760
This article has not been copyedited and formatted. The final version may differ from this version.

The spectrum in the presence of PE was assumed to represent background noise and this was subtracted from the control spectrum obtained prior to superfusion with PE to obtain the spectrum of the PE-sensitive current. The PE-sensitive spectra were fitted by a single Lorentzian function:

$$S(f) = \frac{S(0)}{1 + (f/f_c)^2}, \quad (8)$$

where S(0) is a constant with units of A^2s, f represents frequency (Hz) and f_c is the corner frequency (Dempster, 1993). The current variance was calculated from the integral of this function:

$$\sigma^2 = \frac{\pi f_c S(0)}{2}. \quad (9)$$

Assuming that the PE-sensitive current represented a single population of K^+-selective channels gating between a single closed state and open state with an open probability ≤ 0.1, the single channel conductance was calculated as:

$$\gamma = \frac{\sigma^2}{\Delta I(V_m - E_K)}, \quad (10)$$

where ΔI is the portion of the macroscopic steady-state current inhibited by PE, V_m is the pulse potential (*ie* +40mV) and E_K is the equilibrium potential for K^+ ions in these experiments (~-95mV) (Dempster, 1993, Helliwell and Large, 1998).

Statistics

Data are presented as the mean ± S.E.M. Current-voltage relations were analyzed by two-way analysis of variance. All other results were analyzed by paired or unpaired *t*-tests ($p < 0.05$ were considered significant).

Molecular Pharmacology Fast Forward. Published on June 24, 2004 as DOI: 10.1124/mol.104.000760
This article has not been copyedited and formatted. The final version may differ from this version.

RESULTS

Phenylephrine inhibits a time-independent outward current

Using the perforated patch whole cell voltage-clamp technique, membrane depolarization positive to –50mV elicited outward currents that activated rapidly to a peak and then partially inactivated over the course of 1s pulses (Fig. 1A). Superfusion with the α_1-AR agonist, phenylephrine (PE; 10μM) reduced the amplitude of the outward currents (Fig. 1A). Current-voltage relations from 7 cells, in the absence and presence of PE, are shown in Fig. 1B. PE significantly reduced both the mean peak and late outward currents from voltages positive to -50mV (Fig. 1B). PE had no effect on the inward currents negative to –80mV, indicating that α_1-ARs did not modulate I_{K1} under these conditions. The reduction of both peak and late outward current is consistent with the inhibition by PE of a time-independent outward current. To substantiate this, outward current from –50mV and positive was fitted with a double exponential relation and the conductance of the time-independent component (A_0) calculated assuming K^+ selectivity. The voltage-dependence of the conductance density from voltages positive to –50mV is shown in Fig. 1C and clearly demonstrates that PE reduced a time-independent conductance that was independent of voltage over this range of membrane potentials.

To investigate the nature of the PE-sensitive current further, the dependence of outward current on conditioning potential (CP) was examined (Fig. 2A). For each of 7 cells, the current evoked on depolarization to +40mV was plotted against the preceding CP both under control conditions and in the presence of 10μM PE; an example is shown in Figure 2B. The peak outward current showed marked voltage-dependent inactivation but significant current remained even from depolarized CP, suggesting the existence of inactivating transient (I_t) and non-inactivating steady-state (I_{ss}) outward currents in these cells (Fig. 2B). The mean

Molecular Pharmacology Fast Forward. Published on June 24, 2004 as DOI: 10.1124/mol.104.000760
This article has not been copyedited and formatted. The final version may differ from this version.

± S.E.M of fitted parameters from a single Boltzmann equation for the 7 cells are shown in Table 1. It is clear that the predominant and most significant effect of PE was inhibition of I_{ss}, with no significant effect on I_t under these conditions (Table 1). It is worth noting that in 4 of the 7 cells, including the example shown in Figs. 2A & 2B, the voltage-dependent inactivation of the currents could be fitted by a double Boltzmann equation (mean $V_{0.5,1}$ for I_{to1} = -50.6 ± 1.9mV, mean $V_{0.5,2}$ for I_{Kx} = -18.9 ± 3.1mV). In these cells, in addition to inhibition of I_{ss} (from 6.92 ± 1.21 pA/pF to 5.41 ± 0.97 pA/pF, P<0.02, *n*=4), PE inhibited I_{to1} from 12.60 ± 2.12 pA/pF to 7.39 ± 0.85 pA/pF (P<0.05). In contrast, the amplitude of I_{Kx} was slightly, but not significantly, increased by PE (from 2.52 ± 0.68 pA/pF to 3.75 ± 1.32 pA/pF, p<0.09, *n*=4). On the other hand, PE did not significantly affect the parameters of voltage-dependent inactivation of I_{to1} or I_{Kx}.

The time course of inactivation of the currents activated on depolarization to +40mV from a CP of –70mV (1s) was fitted by a double exponential equation (Fig. 2A). PE affected neither the time constants of inactivation nor the amplitude of the inactivating current components, A_1 and A_2. Figure 2C shows the mean amplitudes of the inactivating current (calculated as A_1+A_2) and the time-independent current (A_0). Clearly, PE had no effect on the total inactivating current but it inhibited markedly the time-independent current, A_0 (Fig. 2C). Consistent with the voltage-dependent inactivation of I_t (Fig. 2B & Table 1), from a CP of 0mV the amplitude of the inactivating current was considerably reduced compared to that from a CP of -70mV and the time course of inactivation was fitted by a single exponential equation (Figs. 2A & 2C). Once again, PE significantly inhibited the time-independent current but was without effect on the inactivating current (Fig. 2C). Most significantly, the PE-sensitive current, calculated as the difference between the A_0 component before and during superfusion with PE, was independent of the conditioning potential (CP = -70 mV:

Molecular Pharmacology Fast Forward. Published on June 24, 2004 as DOI: 10.1124/mol.104.000760
This article has not been copyedited and formatted. The final version may differ from this version.

1.69 ± 0.39 pA/pF; CP = 0mV: 1.75 ± 0.69 pA/pF, *n*=7). Taken together, these results indicate that PE inhibited a steady-state outward current.

The PE-sensitive current is a K^+-selective, time-independent current

The properties of the PE-sensitive current were investigated in detail using conventional whole cell voltage-clamp recording. PE (10μM) did not alter the inactivating components of the current, but markedly reduced the time-independent A_0 component by 2.32 ± 0.25 pA/pF (*n*=44; p<<0.0001 paired *t*-test, Fig. 3A). PE reduced the amplitude of outward currents measured at the end of 500ms pulses to +40mV by 2.26 ± 0.23 pA/pF (*n*=44), the effect reaching a steady-state within 4 min (Fig. 3B). The close correspondence between this value and the PE-sensitive current measured as the A_0 component (2.32 pA/pF) confirms that the predominant current modulated by PE in these cells was a time-independent current. Indeed, subtraction of the currents in the presence of PE from the control currents revealed the time-independent nature of the PE-sensitive current (Fig. 3A). Replacement of pipette K^+ with the monovalent cations Cs^+ or Li^+ markedly reduced the outward currents (*cf.* Figs. 3C and 3D with Fig. 3A, note the difference in scale) and effectively abolished the response to PE (Fig. 3E). Thus, PE inhibited a time-independent K^+-selective outward current.

The effect of internal TEA on the PE-sensitive current

Many K_v channels are blocked at the internal mouth of the pore by the voltage-gated K^+ channel blocker, tetraethylammonium (TEA) (Snyders, 1999). To characterize the outward currents further, the effects were investigated of incorporation of TEA (20mM) in the pipette solution on the currents elicited from CP of –70mV and 0mV (Figs 4A & 4B). Although internal TEA considerably reduced the inactivating (A_1+A_2) currents activated from a CP of –70mV, there was no effect on the time-independent A_0 (Figs. 4C). From a CP of

Molecular Pharmacology Fast Forward. Published on June 24, 2004 as DOI: 10.1124/mol.104.000760
This article has not been copyedited and formatted. The final version may differ from this version.

0mV the A_1+A_2 currents were largely inactivated and internal TEA had no effect on either the residual inactivating or time-independent currents (Fig. 4D), demonstrating that internal TEA blocked I_t selectively with no effect on I_{ss}. Moreover, even in the presence of internal TEA, PE markedly inhibited A_0 (Fig. 4E) such that the PE-sensitive current was unaffected by internal TEA (Fig. 4F). Therefore, internal TEA differentiated between PE-sensitive and time-dependent current components.

The effects of external acidosis and TASK channel blockers on the outward currents

The effect on the PE-sensitive current of acute reduction of extracellular pH from 7.35 to 6.1 was determined. Cells were superfused with low pH for 90-100s before administration of 10μM PE. Extracellular acidosis differentially affected inactivating and non-inactivating currents (Figs. 5A & 5B). The amplitude of the inactivating current (A_1+A_2) was markedly increased, while A_0 was slightly, but not significantly reduced (Fig. 5B). However, the inhibitory effect of PE on the time-independent current (A_0) was almost abolished at low pH (Figs. 5B & 5E). TASK-1 K^+ channel currents have been shown to be blocked by the arachidonic acid derivative, anandamide, whilst TASK-3 channels are blocked by the cationic dye, ruthenium red (Czirjak and Enyedi, 2003, Maingret et al., 2001). Superfusion of myocytes with anandamide (10μM) markedly reduced A_0, with no significant effect on A_1+A_2 (Fig. 5C). Application of PE in the presence of anandamide further decreased A_0 (Fig. 5C). In contrast, ruthenium red (20μM) had no significant effect on either A_0 or A_1+A_2 (Fig. 5D). Thus, the PE-sensitive current was partially reduced by anandamide while ruthenium red had no effect (Fig. 5E). TASK-1 channels have been shown to be blocked by external Zn^{2+} and Ba^{2+} (Duprat et al., 1997, Kim et al., 1999, Leonoudakis et al., 1998). Superfusion with 1mM $ZnCl_2$ significantly inhibited the A_0 component and increased the amplitude of the A_1+A_2 component, although the latter effect did not reach statistical significance (Fig. 6A; p=0.053, *n*=9). However, Zn^{2+} did not affect the PE-sensitive current (Fig. 6C). In contrast, 10mM

Molecular Pharmacology Fast Forward. Published on June 24, 2004 as DOI: 10.1124/mol.104.000760
This article has not been copyedited and formatted. The final version may differ from this version.

$BaCl_2$ strongly inhibited both the A_0 and A_1+A_2 components and markedly reduced the PE-sensitive current (Figs. 6B & 6C).

The effect of K^+ channel blockers on the PE-sensitive current

4-aminopyridine (4-AP) and TEA, applied externally, have been reported to inhibit partially I_{ss} in rat ventricular myocytes (Apkon and Nerbonne, 1991, Himmel et al., 1999). Consistent with these reports, 4-AP was found to inhibit concentration-dependently the A_0 component, producing a maximal inhibition of ~20% reduction from control at 10mM (Fig. 7A). In contrast, 10mM 4-AP reduced the inactivating component (A_1+A_2) by 82.5% ± 6.1% of control (*n*=8). Most notably, in the presence of 10mM 4-AP, the response to 10μM PE was reduced to approximately 45% of control (Figs. 7B & 7C). 10mM external TEA also partially inhibited the time-independent A_0 component (20.3% ± 6.9%, *n*=6; Fig 8A). However, in contrast to the action of 4-AP, 10mM TEA did not significantly affect the inactivating current (Fig. 8A). In the presence of 50mM external TEA, both the A_0 and the A_1+A_2 components were markedly reduced from control (Fig. 8B). The PE-sensitive current was significantly reduced in the presence of 10mM and 50mM external TEA (Fig. 8C).

The effect of PE on the power spectrum of current noise

During the course of these experiments it was noted that the noise of outward whole cell currents was generally reduced in the presence of 10μM PE (Fig. 9A). Since it was conceivable that the inhibitory effect of PE on the whole cell currents might be associated with the inhibition of activity of K^+ channels of relatively large unitary conductance, a spectral analysis of the current noise was conducted on 8 cells that fell within our exclusion criterion (see Methods). Figure 9B shows the power spectra for the currents shown in Figure 9A in the absence and presence of 10μM PE. As expected from visual inspection of the current traces (*e.g.* Fig. 9A), the power of the noise at frequencies of 7.8Hz and above was

Molecular Pharmacology Fast Forward. Published on June 24, 2004 as DOI: 10.1124/mol.104.000760
This article has not been copyedited and formatted. The final version may differ from this version.

consistently reduced in the presence of PE (Fig. 9B). The power spectrum in the presence of PE was assumed to represent background noise and was subtracted from the control power spectrum to give the power spectrum of the PE-sensitive current. The power spectrum of the PE-sensitive current was fitted with a single Lorentzian (equation 8) with mean S(0) = 25.4 ± 9.2 pA^2s and mean f_c = 116 ± 20 Hz (n=8). Assuming that the PE-sensitive current represented a single population of K^+-selective channels, the mean single channel conductance (γ) calculated according to equation 10 was 77.9 ± 4.3 pS (n=8). We were concerned that with the exclusion criteria used, the attenuation of the power spectrum at frequencies above the cut-off frequency, f_{RC}, might lead to error in the estimation of the single channel conductance. However, if this were the case, it might be expected that there should be a correlation between the value of f_{RC} and the single channel conductance. No such relation existed. Thus, the above estimate of single channel conductance was not different from that obtained using 3 of these cells that fulfilled more stringent exclusion criteria (τ_m < 500μs, f_{RC} ranging from 345 – 400 Hz) in which mean S(0) = 14.7 ± 6.1 pA^2s, mean f_c = 140 ± 10 Hz, corresponding to a mean single channel conductance of 75.8 ± 5.9 pS.

The effect of quinidine on the PE-sensitive current: evidence for involvement of Slick

The high unitary conductance of the PE-sensitive current (Fig. 9) and its partial sensitivity to external 4-AP (Fig. 7) and TEA (Fig. 8) are reminiscent of Slick voltage-gated K^+ channels (Bhattacharjee et al., 2003). Since Slick channels are blocked by external administration of high concentrations of quinidine, the effect on the PE-sensitive current of this anti-arrhythmic drug was examined (Fig. 10). Quinidine (100μM) inhibited the time-dependent A_1+A_2 component by 70.7 ± 12.4% and the time-independent A_0 component by 58.4 ± 3.4% (n=6, Figs. 10A and 10B). Moreover, in the presence of 100μM quinidine, the PE-sensitive time-independent current was markedly and significantly reduced (Fig. 10C). The inhibitory response to PE was effectively abolished by 1mM quinidine, although there

Molecular Pharmacology Fast Forward. Published on June 24, 2004 as DOI: 10.1124/mol.104.000760
This article has not been copyedited and formatted. The final version may differ from this version.

was also evidence of non-specific actions on the whole-cell membrane current at this very high concentration (*n*=5, data not shown).

Slick channel activity is reported to be increased by very high concentrations of Na^+ (*i.e.* >20mM; EC_{50}=81mM, nH=1.4) at the cytosolic surface of excised membrane patches from chinese hamster ovary cells transfected with the Slick cDNA (Bhattacharjee et al., 2003). No information is available regarding the Na^+-sensitivity of native Slick channels (either from excised patches or whole-cell recordings) from any cell type. Estimates of intracellular [Na^+] in rat ventricular myocytes range from 10-20mM, depending on the recording conditions and stimulation frequency (Despa et al., 2002). Therefore, the effect on the PE-sensitive current of dialyzing the cells with a pipette solution containing a concentration of Na^+ at the upper end of the physiological range was investigated. However, the amplitude of the PE-sensitive current recorded with a pipette [Na^+] = 20mM (1.75 ± 0.47 pA/pF, *n*=7) was not significantly different from that recorded under control conditions. Thus, the PE-sensitive current was insensitive to intracellular Na^+ in the physiological concentration range. Since the sensitivity of Slick channels in excised inside-out patches to Na^+ at the cytosolic surface of the patch operates in a supra-physiological range of concentrations, this observation does not preclude the involvement of Slick channels to the PE-sensitive current.

The involvement of α_1-ARs in current modulation

The response to PE was effectively abolished in the presence of the α_1-AR antagonist, prazosin (1μM, Fig. 11A). However, pre-treatment of the cells with the site-specific alkylating reagent, chloroethylclonidine (CEC), which modifies α_{1B}- and α_{1D}- but not α_{1A}-ARs (Zhong and Minneman, 1999), did not attenuate the response to PE (Figs. 11A & B). Indeed, PE produced a similar effect in CEC pre-treated cells to that observed in control cells

Molecular Pharmacology Fast Forward. Published on June 24, 2004 as DOI: 10.1124/mol.104.000760
This article has not been copyedited and formatted. The final version may differ from this version.

(*cf*. Fig. 11B with Fig. 3A). The α_{1A}-AR specific antagonist, WB4101, almost completely abolished the response to PE, in a manner similar to prazosin (Fig. 11A), suggesting that the response to PE was mediated predominantly by α_{1A}-ARs. Furthermore, the α_{1A}-specific agonist, A61603, inhibited a time-independent current in a manner similar to PE (Figs. 11A & 11C).

Investigation of the signaling pathways involved in the PE-response

α_1-adrenoceptors activate multiple intracellular signaling pathways, principally involving G_q GTP-binding proteins, although they have also been reported to couple to PTX-sensitive G-proteins (Fedida et al., 1993a, Zhong and Minneman, 1999). The response to PE was considerably reduced in cells in which intracellular GTP was depleted by including GDPβS in the pipette solution (Fig. 12A). On the other hand, the response to PE was not reduced by pre-incubation of cells with pertussis toxin (PTX) for at least 1 hr at 37^{o}C (Fig. 12A). The inhibition of $G_{i/o}$-mediated pathways in the PTX-treated cells was confirmed by examining the action of the muscarinic agonist, carbachol, on $I_{Ca,L}$ in the presence of the β-AR agonist, isoprenaline (data not shown). On the other hand, incorporation in the pipette of the G_q-antagonist peptide, GP2A (Mukai et al., 1992), slightly but significantly inhibited the response to PE (Fig. 12A). Strongly buffering intracellular Ca^{2+} using BAPTA had no effect on the PE response (Fig. 12A). In contrast, pre-treatment of the cells for 10 min with a widely used inhibitor of phospholipase C (PLC), U73122 (5μM), reduced the effect of PE (Fig. 12B). However, this effect of U73122 was not significantly different from that of its inactive analog, U73343 (5μM). Moreover, the non-selective inhibitor of PLC and phospholipase D (PLD), neomycin, had no effect on the responses to PE (Fig. 12B) (Liscovitch et al., 1991). Similarly, although treatment of the cells with 40μM $AACOCF_3$, a phospholipase A_2 (PLA_2) inhibitor, significantly reduced the response to PE, an alternative PLA_2 inhibitor, MAFP (25μM), had no effect (Fig. 12B). Interventions targeted at protein kinase C (PKC) did not

Molecular Pharmacology Fast Forward. Published on June 24, 2004 as DOI: 10.1124/mol.104.000760
This article has not been copyedited and formatted. The final version may differ from this version.

significantly affect the response to PE (Fig. 12C). Although the response to PE was significantly reduced by the tyrosine kinase inhibitor, genistein (50μM), the control currents prior to administration of PE were also reduced. Thus, a non-specific action of the isoflavone on the steady-state current cannot be ruled out (Fig. 12C). On the other hand, intracellular administration of the phosphatidylinositol 3-kinase (PI 3-kinase) inhibitor, 5μM wortmannin, significantly reduced the response to PE but not the control current (Fig. 12C).

DISCUSSION

This report demonstrates that PE inhibits a K^+-selective current with properties distinct from other cardiac currents characterized to date (Snyders, 1999). Moreover, the data show that the inhibitory response to PE was mediated predominantly through α_{1A}-adrenoceptors, via a pathway involving PTX-insensitive G-proteins and PI 3-kinase but independent of cytosolic Ca^{2+} and phospholipase C.

The predominant current modulated by PE is a K^+-selective steady-state current

Two lines of evidence demonstrate that the A_0 and the A_1+A_2 components obtained by curve-fitting represent distinct K^+ channel types: (1) The A_1+A_2 components were markedly reduced (~16-fold) by conditioning pulses to 0mV whereas the A_0 component was unaffected (Figs. 2A & 2C); (2) the A_1+A_2 currents were effectively (~17-fold) and selectively inhibited by incorporation of the voltage-gated K^+ channel blocker, TEA, in the pipette solution (Fig. 4), whereas the PE-sensitive current was insensitive to internal TEA but was K^+-selective (Figs. 3E & 4F). The notion that a steady-state current represents the predominant current modulated by PE was supported by Boltzmann analysis of voltage-dependent inactivation (Fig. 2 & Table 1). These data are consistent with the propositions that: (a) the sum of the A_1 and A_2 components represents I_t; (b) that Kv1.x and Kv4.x

Molecular Pharmacology Fast Forward. Published on June 24, 2004 as DOI: 10.1124/mol.104.000760
This article has not been copyedited and formatted. The final version may differ from this version.

channels contribute to I_t in these cells, and (c) that A_0 represents a steady-state K^+ current, I_{ss}, distinct from I_t (Himmel et al., 1999, Snyders, 1999).

Previously, α_1-ARs have been reported to inhibit cardiac I_{to1} (Fedida et al., 1993a). Considerable heterogeneity exists between cells in the relative contribution of sub-components of the transient outward current (Himmel et al., 1999, Snyders, 1999) and we do not exclude the possibility that α_1-ARs are able to modulate I_{to1} under some experimental conditions. For example, in experiments performed using the perforated patch recording technique, the voltage-dependent inactivation of the currents in a subset of the cells could be fitted by a double Boltzmann equation (Fig. 2) according to (Himmel et al., 1999). In these 4 cells, I_{to1} (but not I_{Kx}) was significantly inhibited by PE in addition to I_{ss}. Nevertheless, the predominant effect of PE in experiments performed using either the perforated patch (*n*=7; Fig. 2) or conventional whole cell (*n*=44; Fig. 3) recording techniques was the inhibition of a time-independent outward current (A_0) with no significant overall effect on the inactivating currents (A_1+A_2). It is therefore possible to attribute with confidence the observed effects of α_1-AR activation on A_0 to effects on I_{ss} rather than on I_t.

Properties of the PE-sensitive current ($I_{ss,PE}$)

The power spectrum of the PE-sensitive current noise could be fitted by a single Lorentzian component (Fig. 9), an observation consistent with the contribution of a single population of channels to the PE-sensitive current (Dempster, 1993). Assuming a linear open channel current-voltage relation for a single population of K^+-selective channels, the unitary channel conductance was estimated to be ~78pS (Fig. 9). However, on the basis of the data shown in Figures 6 – 10, the possibility that the PE-sensitive current represents a heterogeneous current of more than one population of channels cannot be entirely excluded. Nevertheless, although the unitary conductance would be under-estimated in that case, the

Molecular Pharmacology Fast Forward. Published on June 24, 2004 as DOI: 10.1124/mol.104.000760
This article has not been copyedited and formatted. The final version may differ from this version.

noise analysis suggests the contribution of a channel of at least 78pS to the PE-sensitive current. The absence of effect of PE on the inward currents at potentials negative to E_K (Fig. 1B) indicates that the PE-sensitive current shows outward rectification, consistent with the involvement of a voltage-dependent channel. On the other hand, the conductance-voltage relation shows that the PE-sensitive current was fully activated at potentials positive to -50mV (Fig. 1C). Although no inactivation of $I_{ss,PE}$ could be observed in the present study (Figs. 2 & 3), our data do not exclude the possibility that the PE-sensitive current inactivates very slowly (time constant >1s). In summary, $I_{ss,PE}$ represents a current through a rapidly activating K^+ channel with unitary conductance of at least 78pS that produces an outwardly rectifying current that either does not inactivate or inactivates only very slowly.

The lack of inhibition of the PE-sensitive current by internal TEA, which can be expected to block the voltage-gated K^+ channel α-subunits thought to underlie cardiac I_{Kur} (Fedida et al., 1996, Nattel et al., 1999, Shieh and Kirsch, 1994, Taglialatela et al., 1994), is inconsistent with the suggestion (van Wagoner et al., 1996, Nattel et al., 1999) that $I_{ss,PE}$ represents a subtype of I_{Kur} (Fig. 3F). Moreover, both control I_{ss} and the PE-sensitive current were only partially inhibited by relatively high concentrations of 4-AP (Fig. 7), which would be expected to completely block I_{Kur} (Nattel et al., 1999). Furthermore, the unitary conductances reported for the Kv1.5, Kv1.2, Kv2.1 or Kv3.1 I_{Kur} channels (13 – 25pS) are much lower than $I_{ss,PE}$ (Fedida et al., 1993b, Shahidullah et al., 1995, Shieh and Kirsch, 1994, Taglialatela et al., 1994). Taken together, our data suggest that the inhibitory response to PE involves a current distinct from I_{Kur}.

Although acute acidosis reduced the inhibitory response to PE by ~88% (Fig. 5E), the control time-independent current was not significantly reduced by acidosis (Fig. 5B); a finding inconsistent with the involvement of acid-sensitive K^+ channels in the PE-sensitive

Molecular Pharmacology Fast Forward. Published on June 24, 2004 as DOI: 10.1124/mol.104.000760
This article has not been copyedited and formatted. The final version may differ from this version.

current. At concentrations sufficient to produce complete block of TASK-1 channels, anandamide (10μM; (Maingret et al., 2001) produced only partial inhibition of the PE response while Zn^{2+} (Leonoudakis et al., 1998) was without effect (Figs. 5 & 6). The TASK-3 inhibitor, ruthenium red, also had no effect (Fig. 5E). Moreover, the biophysical properties of the PE-sensitive current are quite distinct from TASK-1: TASK-1 channels have a unitary conductance of 14pS (Kim et al., 1999) and produce 'leak' background K^+ currents that pass inward current negative to E_K (Duprat et al., 1997). Thus, taken together, our data do not support a predominant role for TASK channels in the PE response. Three properties of I_{ss} are inconsistent with the involvement of TREK: (1) the inhibitory response to PE was observed in the absence of either membrane stretch or exogenous polyunsaturated fatty acids; (2) TREK is insensitive to external TEA; (3) TREK-1 has a unitary conductance of 48pS in physiological external [K^+] (Patel et al., 1998).

Slick – a possible molecular basis to $I_{ss,PE}$?

Slick is a very recently identified slo-type voltage-gated K^+ channels that is expressed in the heart (Bhattacharjee et al., 2003). But no native Slick-like cardiac current has yet been identified. The PE-sensitive current characterized in this study resembles Slick K^+ channel currents in respect of a large unitary conductance (Fig. 9), outward rectification (Fig. 1C), maximal activation at potentials positive to –50mV (Fig. 1C), time-independence (Fig. 3), partial sensitivity to high concentrations of external TEA (Fig. 8) and sensitivity to external Ba^{2+} and quinidine (Figs. 6 & 10) (Bhattacharjee et al., 2003). Moreover, slo channels are relatively insensitive to blockade by internal TEA (Moss and Magleby, 2001). These similarities suggest that further work is now required to establish the contribution of Slick to $I_{ss,PE}$.

Molecular Pharmacology Fast Forward. Published on June 24, 2004 as DOI: 10.1124/mol.104.000760
This article has not been copyedited and formatted. The final version may differ from this version.

PE acts predominantly via α_{1A}-ARs acting through a PTX-insensitive G-protein

The effect of prazosin on the response to PE confirms the involvement of α_1-adrenoceptors in modulation of I_{ss} (Fig. 11A). The lack of effect on the responses to PE of pre-treatment with α_{1B}-AR and α_{1D}-AR selective inhibitor and the marked inhibition by the α_{1A}-AR selective antagonist, WB4101, suggest that the responses to PE were predominantly mediated via the α_{1A}-AR (Figs. 11A & 11B). This conclusion is supported by the inhibitory effect of the α_{1A}-AR agonist, A61603 on I_{ss} (Figs. 11A & 11C). The marked attenuation of the PE-sensitive current in GDPβS-dialyzed cells and the lack of effect of PTX demonstrated the involvement of PTX-insensitive G-proteins, presumably G_q, in the response to the α_1-agonist (Fig. 12A). The inhibitory effect of the antagonist peptide, GP2A, on the response to PE is consistent with this conclusion (Fig. 12A). The results with U73122 and U73343 and the lack of effect of neomycin suggest that the actions of PE did not involve PLC or PLD, consistent with the observation of robust responses to PE when bulk cytosolic Ca^{2+} was chelated to <1nM with BAPTA (Singer et al., 1997). Since $AACOCF_3$ is known to have non-specific actions independent of PLA_2 inhibition (Fonteh, 2002) and MAFP had no significant effect on the responses to PE (Fig. 12B), there is no consistent evidence for the involvement of PLA_2. On the other hand, the inhibitory effect of wortmannin on the PE response suggests the involvement of PI 3-kinase (Fig. 12C).

Conclusions and implications

It is well established that α_1-AR stimulation modulates the electrophysiology of cardiac myocytes from different regions of the heart in a number of species (*e.g.* dog, ferret, rabbit, rat, human *etc*), including rat ventricular myocytes (Fedida et al., 1993a, Li et al., 1996). Since $I_{ss,PE}$ represented the predominant current modulated by α_1-ARs in the present study, it seems likely to play an important role in the modulation of excitability and refractoriness in these cells. This current could therefore represent a potential target for anti-

Molecular Pharmacology Fast Forward. Published on June 24, 2004 as DOI: 10.1124/mol.104.000760
This article has not been copyedited and formatted. The final version may differ from this version.

arrhythmic agents and further work is warranted to establish the contribution of this Slick-like K^+ channel current to cardiac excitability and repolarization.

ACKNOWLEDGEMENTS

Thanks to Dr Zhiwei Cai (Bristol) for discussion of noise analysis.

REFERENCES

Aimond F, Rauzier J-M, Bony C and Vassort G (2000) Simultaneous Activation of p38 MAPK and p42/44 MAPK by ATP Stimulates the K^+ Current I_{TREK} in Cardiomyocytes. *Journal of Biological Chemistry* 275:39110-39116.

Apkon M and Nerbonne JM (1991) Characterization of two distinct depolarization-activated K^+ curents in isolated adult rat ventricular myocytes. *Journal of General Physiology* 97:973-1011.

Backx PH and Marban E (1993) Background potassium current active during the plateau of the action potential in guinea pig ventricular myocytes. *Circulation Research* 72:890-900.

Barbuti A, Ishii S, Shimizu T, Robinson RB and Feinmark SJ (2002) Block of the background K^+ channel TASK-1 contributes to arrhythmogenic effects of platelet-activating factor. *American Journal of Physiology* 282:H2024-H2030.

Bhattacharjee A, Joiner WJ, Wu M, Yang Y, Sigworth FJ and Kaczmarek LK (2003) Slick (Slo2.1), a Rapidly-Gating Sodium-Activated Potassium Channel Inhibited by ATP. *Journal of Neuroscience* 23:11681-11691.

Czirjak G and Enyedi P (2003) Ruthenium Red Inhibits TASK-3 Potassium Channel by Interconnecting Glutamate 70 of the Two Subunits. *Molecular Pharmacology* 63:646-652.

Dempster J (1993) Analysis of ionic current fluctuations: noise analysis, in *Computer analysis of electrophysiological signals* eds) pp 191-203, Academic Press, London.

Despa S, Islam MA, Pogwizd SM and Bers DM (2002) Intracellular [Na^+] and Na^+ pump rate in rat and rabbit ventricular myocytes. *Journal of Physiology (London)* 539:133-143.

Duprat F, Lesage F, Fink M, Reyes R, Heurteaux C and Lazdunski M (1997) TASK, a human background K^+ channel to sense external pH variations near physiological pH. *The EMBO Journal* 16:5464-5471.

Ertl R, Jahnel U, Nawrath H, Carmeliet E and Vereecke J (1991) Differential electrophysiologic and inotropic effects of phenylephrine in atrial and ventricular heart muscle preparations from rats. *Naunyn-Schmiedeberg's Archives of Pharmacology* 344:574-581.

Fedida D, Bouchard R and Chen FS (1996) Slow gating charge immobilization in the human potassium channel Kv1.5 and its prevention by 4-aminopyridine. *Journal of Physiology (London)* 494:377-387.

Fedida D, Braun AP and Giles WR (1993a) α_1-adrenoceptors in myocardium: functional aspects and transmembrane signaling mechanisms. *Physiological Reviews* 73:469-487.

Fedida D, Wible B, Wang Z, Fermini B, Faust F, Nattel S and Brown AM (1993b) Identity of a novel delayed rectifier current from human heart with a cloned K^+ channel current. *Circulation Research* 73:210-216.

Fonteh AN (2002) Differential effects of arachidonoyl trifluoromethyl ketone on arachidonic acid release and lipid mediator biosynthesis by human neutrophils: Evidence for different arachidonate pools. *European Journal of Biochemistry* 269:3760-3770.

Helliwell RM and Large WA (1998) Facilitatory effect of Ca^{2+} on the noradrenaline-evoked cation current in rabbit portal vein smooth muscle cells. *Journal of Physiology (London)* 512:731-741.

Himmel HM, Wettwer E, Li Q and Ravens U (1999) Four different components contribute to outward current in rat ventricular myocytes. *American Journal of Physiology* 277:H107-H118.

Homma N, Hirasawa A, Shibata K, Hashimoto K and Tsujimoto G (2000) Both α_{1A}- and α_{1B}-adrenergic receptor subtypes couple to the transient outward current (I_{To}) in rat ventricular myocytes. *British Journal of Pharmacology* 129:1113-1120.

Jones SA, Morton MJ, Hunter M and Boyett MR (2002) Expression of TASK-1, a pH-sensitive twin-pore domain K^+ channel, in rat myocytes. *American Journal of Physiology* 283:H181-H185.

Kim Y, Bang H and Kim D (1999) TBAK-1 and TASK-1, two-pore K^+ channel subunits: kinetic properties and expression in rat heart. *American Journal of Physiology* 277:H1669-H1678.

Leonoudakis D, Gray AT, Winegar BD, Kindler CH, Harada M, Taylor DM, Chavez RA, Forsayeth JR and Yost CS (1998) An open rectifier potassium channel with two pore domains in tandem cloned from rat cerebellum. *Journal of Neuroscience* 18:868-878.

Lesage F and Lazdunski M (2000) Molecular and functional properties of two-pore-domain potassium channels. *American Journal of Physiology* 279:F793-801.

Li G-R, Feng J, Wang Z, Fermini B and Nattel S (1996) Adrenergic Modulation of Ultrarapid Delayed Rectifier K^+ Current in Human Atrial Myocytes. *Circulation Research* 78:903-915.

Liscovitch M, Chalifa V, Danin M and Eli Y (1991) Inhibition of neural phospholipase D activity by aminoglycoside antibiotics. *Biochemical Journal* 279:319-321.

Maingret F, Patel AJ, Lazdunski M and Honore E (2001) The endocannabinoid anandamide is a direct and selective blocker of the background K^+ channel TASK-1. *EMBO Journal* 20:47-54.

Millar JA, Barratt L, Southan AP, Page KM, Fyffe REW, Robertson B and Mathie A (2000) A functional role for the two-pore domain potassium channel TASK-1 in cerebellar granule neurons. *Proceedings of the National Academy of Sciences USA* 97:3614-3618.

Moss BL and Magleby KL (2001) Gating and Conductance Properties of BK Channels Are Modulated by the S9-S10 Tail Domain of the α Subunit: A Study of mSlo1 and mSlo3 Wild-type and Chimeric Channels. *Journal of General Physiology* 118:711-734.

Mukai H, Munekata E and Higashijima T (1992) G protein antagonists. A novel hydrophobic peptide competes with receptor for G protein binding. *Journal of Biological Chemistry* 267:16237-16243.

Nattel S, Yue L and Wang Z (1999) Cardiac ultrarapid delayed rectifiers: A novel potassium current family of functional similarity and molecular diversity. *Cellular Physiology and Biochemistry* 9:217-226.

Patel AJ, Honore E, Maingret F, Lesage F, Fink M, Duprat F and Lazdunski M (1998) A mammalian two pore domain mechano-gated S-like K^+ channel. *EMBO Journal.* 17:4283-4290.

Ravens U, Wang X-L and Wettwer E (1989) Alpha adrenoceptor stimulation reduces outward currents in rat ventricular myocytes. *Journal of Pharmacology and Experimental Therapeutics* 250:364-370.

Shahidullah M, Hoshi N, Yokoyama S, Kawamura T and Higashida H (1995) Slow inactivation conserved in heteromultimeric voltage-dependent K+ channels between Shaker (Kv1) and Shaw (Kv3) subfamilies. *FEBS Letters* 371:307-310.

Shieh CC and Kirsch GE (1994) Mutational analysis of ion conduction and drug binding sites in the inner mouth of voltage-gated K^+ channels. *Biophysical Journal* 67:2316-2325.

Singer WD, Brown HA and Sternweis PC (1997) Regulation of eukaryotic phosphatidylinositol-specific phospholipase C and phospholipase D. *Annual Review of Biochemistry* 66:475-509.

Snyders DJ (1999) Structure and function of cardiac potassium channels. *Cardiovascular Research* 42:377-390.

Taglialatela M, Champagne M, Drewe J and Brown A (1994) Comparison of H5, S6, and H5-S6 exchanges on pore properties of voltage-dependent K^+ channels. *Journal of Biological Chemistry* 269:13867-13873.

Talley EM, Lei Q, Sirois JE and Bayliss DA (2000) TASK-1, a two-pore domain K^+ channel, is modulated by multiple neurotransmitters in motoneurons. *Neuron* 25:399-410.

Terrenoire C, Lauritzen I, Lesage F, Romey G and Lazdunski M (2001) A TREK-1-Like Potassium Channel in Atrial Cells Inhibited by β-Adrenergic Stimulation and Activated by Volatile Anesthetics. *Circulation Research* 89:336-342.

van Wagoner DR, Kirian M and Lamorgese M (1996) Phenylephrine suppresses outward K^+ currents in rat atrial myocytes. *American Journal of Physiology* 271:H937-H946.

Wang H, Yang B, Zhang Y, Han H, Wang J, Shi H and Wang Z (2001) Different Subtypes of alpha 1-Adrenoceptor Modulate Different K^+ Currents via Different Signaling Pathways in Canine Ventricular Myocytes. *Journal of Biological Chemistry* 276:40811-40816.

Zhong H and Minneman KP (1999) α_1-Adrenoceptor subtypes. *European Journal of Pharmacology* 375:261-276.

FOOTNOTES

Financial support from the British Heart Foundation (PG/98091 and PG/03/073) and the Wellcome Trust is gratefully acknowledged.

Address for reprint requests: Dr Andrew F James, Department of Physiology and Cardiovascular Research Laboratories, School of Medical Sciences, University of Bristol, University Walk, Bristol, BS8 1TD, United Kingdom.

Tel: +44-117-928-9187; Fax: +44-117-928-8923; e-mail: a.james@bristol.ac.uk

[1]Current address for Dr A Martyn Reynolds: Cairn Research Ltd, Graveney Road, Faversham, Kent, ME13 8UP, U.K.

Molecular Pharmacology Fast Forward. Published on June 24, 2004 as DOI: 10.1124/mol.104.000760
This article has not been copyedited and formatted. The final version may differ from this version.

FIGURE LEGENDS

Figure 1. Phenylephrine inhibits a background current. **A** Representative whole cell current traces recorded using the perforated patch technique from a rat ventricular myocyte in the absence (i) and presence (ii) of 10μM phenylephrine (PE) using the pulse protocol shown lower panel (iii). Holding potential was –80mV. **B** Current density-voltage relations measured at the peak (triangles) and at the end of the pulse (late current; squares) in the absence (filled symbols) and presence (open symbols) of PE. Data are the mean ± S.E.M of 7 cells. Peak and late current-voltage relations in the presence of PE were significantly different from control ($p<0.05$; two-way ANOVA). **C** Conductance density-voltage relations for the time-independent (A_0) component of a double exponential relation fitted to the time course of inactivation of the currents in the absence (closed circles) and presence (open circles) of PE, calculated assuming a K^+-selective conductance. Data are the mean ± S.E.M from 7 cells. Conductance density-voltage relations in the presence of PE were significantly different from control ($p<0.05$; two-way ANOVA).

Figure 2. Phenylephrine inhibits a steady-state outward current. **A** Representative whole cell current traces from differing conditioning potentials (CP) recorded using the perforated patch technique from a rat ventricular myocyte in the absence (upper panel) and presence (middle panel) of 10μM phenylephrine (PE) using the pulse protocol shown (lower panel). Solid lines represent fits to a single exponential (CP=0mV; equation 3) and a double exponential (CP=-70mV, equation 4). Holding potential was –80mV. **B** The effect of CP on steady-state inactivation of peak (triangles) and late (squares) currents in the absence (filled symbols) and presence (open symbols) of PE for the cell shown in A. The solid lines represent fits to a single Boltzmann (equation 1). The $V_{0.5}$ for I_t under control conditions for the data shown was –53.6mV. The dashed lines represent fits to a double Boltzmann (equation 2). The $V_{0.5}$ for I_{to1} and I_{Kx} under control conditions for the data shown were –56.3mV and –27.2mV,

Molecular Pharmacology Fast Forward. Published on June 24, 2004 as DOI: 10.1124/mol.104.000760
This article has not been copyedited and formatted. The final version may differ from this version.

respectively. **C** The effect of CP potential on the mean ± S.E.M of A_0 (upper panel) and A_1+A_2 (lower panel) currents in the absence (solid bars) and presence (hatched bars) of 10μM PE. *: $p<0.05$, paired *t*-test vs control from a CP of 0mV. **: $p<0.01$, paired *t*-test vs control from a CP of –70mV. ††: $p<0.01$, paired *t*-test vs inactivating current from a CP of -70mV.

Figure 3. PE-sensitive current is K^+-selective. **A** Upper panel shows example current traces recorded using the conventional whole cell configuration in the absence and presence of PE using a K^+-rich pipette solution. Solid lines represent fits to a double exponential relation (equation 4). In control, $\tau_1 = 17 \pm 2$ ms and $\tau_2 = 294 \pm 26$ ms (n=44). PE had no significant effect on the τ values. Lower panel shows the PE-sensitive difference current obtained by subtracting the current in the presence of PE from the control current. **B** Time course of inhibition of outward current by 10μM PE. Currents were recorded using a K^+-rich pipette solution and measured at the end of pulses to +40mV (500ms). Holding potential (V_{hold}) was –70mV. Data are the mean ± S.E.M from 44 cells. **C** Upper panel shows example current traces recorded using the Cs^+-rich pipette solution. Current traces in the presence of PE almost completely overlaid control traces. Note the expanded current scale compared to traces shown in A. Lower panel shows PE-sensitive difference current. **D** Upper panel shows example current traces recorded using the Li^+-rich pipette solution. Lower panel shows PE-sensitive difference current. **E** Mean ± S.E.M of PE-sensitive difference currents measured at the end of pulses to +40mV using K^+-rich (n=44), Cs^+-rich (n=6) and Li^+-rich (n=6) pipette solutions. ***: $p<0.001$, unpaired *t*-test vs PE-sensitive difference current with a K^+-rich pipette solution.

Figure 4. Phenylephrine-sensitive current is not blocked by intracellular TEA. **A** Example current traces from conditioning potentials (CP) of –70mV and 0mV recorded using the conventional whole cell configuration and a K^+-rich pipette solution. Solid lines represent fits

Molecular Pharmacology Fast Forward. Published on June 24, 2004 as DOI: 10.1124/mol.104.000760
This article has not been copyedited and formatted. The final version may differ from this version.

to double (CP=-70mV) or single (CP=0mV) exponential equations. **B** Example current traces from conditioning potentials (CP) of –70mV and 0mV recorded using the conventional whole cell configuration and a pipette solution containing 20mM TEA. Solid lines represent fits to double (CP=-70mV; equation 4) or single (CP=0mV; equation 3) exponential relations. **C** Effect of internal TEA (TEA_i) on time-independent (A_0) and inactivating (A_1+A_2) components from a CP of –70mV. Data are the mean ± S.E.M of 7 cells. †: $p<0.05$, un-paired *t*-test vs inactivating current from CP = –70mV recorded using a K^+-rich pipette solution. **D** Effect of TEA_i on time-independent (A_0) and inactivating (A_1+A_2) components from a CP of 0mV. Data are the mean ± S.E.M of 7 cells. *: $p<0.05$, paired *t*-test vs inactivating current from CP = –70mV recorded using a K^+-rich pipette solution. **E** Upper panel shows example current traces recorded using the conventional whole cell configuration in the absence and presence of PE using a pipette solution containing TEA. Solid lines represent a fit to a single exponential relation (equation 3). Lower panel shows the PE-sensitive current obtained by subtracting the current in the presence of PE from the control current. **F** Mean PE-sensitive difference currents calculated by subtracting the A_0 component in the presence of PE from the control. Data represent mean ± S.E.M; numbers in brackets indicate sample sizes. Note that although intracellular TEA markedly inhibited the inactivating current (*cf* B with A), it had no effect on the PE-sensitive current.

Figure 5. Effect on PE-sensitive current of external acidosis and acid-sensitive K^+ channel blockers. **A** Example current traces recorded on depolarization to +40mV at control pH (pH 7.35), at acid pH (pH 6.1) and in the presence of 10μM PE at acid pH. Holding potential was –70mV. Solid lines represent fits to a double exponential relation (equation 4). **B** Mean A_0 and A_1+A_2 components from 7 cells in which external pH was lowered to 6.1. ***: $p<0.001$ paired *t*-test compared with A_1+A_2 at pH 7.35. **C** Mean A_0 and A_1+A_2 components from 7 cells superfused with 10μM anandamide. **: $p<0.01$ paired *t*-test compared with A_0 in the

Molecular Pharmacology Fast Forward. Published on June 24, 2004 as DOI: 10.1124/mol.104.000760
This article has not been copyedited and formatted. The final version may differ from this version.

presence of anandamide alone. **D** Mean A_0 and A_1+A_2 components from 6 cells superfused with 20μM ruthenium red. *: p<0.05 paired *t*-test compared with A_0 in the presence of ruthenium red alone. **E** Mean ± S.E.M of PE-sensitive difference currents calculated by subtracting the A_0 component in the presence of PE from the control under control conditions (C, *n*=44), at an external pH of 6.1 (*n*=7), in the presence of anandamide (An, *n*=7) and in the presence of ruthenium red (RR, *n*=6). †††: p<0.001, unpaired *t*-test vs PE-sensitive difference current under control conditions. ††: p<0.01, unpaired *t*-test vs PE-sensitive difference current under control conditions.

Figure 6. Effect on PE-sensitive current of divalent cations. **A** Upper panel shows example current traces under control conditions, in the presence of 1mM $ZnCl_2$ and in the presence of 1mM $ZnCl_2$ plus 10μM PE. Solid lines represent fits to a double exponential relation (equation 4). Lower panel shows the mean ± S.E.M of the time-independent (A_0) and inactivating (A_1+A_2) currents for 9 cells exposed to 1mM $ZnCl_2$. **: p<0.01, paired *t*-test compared to control. ††: p<0.01, paired *t*-test vs A_0 in the presence of $ZnCl_2$. **B** Upper panel shows example current traces under control conditions, in the presence of 10mM $BaCl_2$ and in the presence of 10mM $BaCl_2$ plus 10μM PE. Solid lines represent fits to a double exponential relation (equation 4). Lower panel shows the mean ± S.E.M of the time-independent (A_0) and inactivating (A_1+A_2) currents for 8 cells exposed to 10mM $BaCl_2$. ***: p<0.001, paired *t*-test vs control. *: p<0.05, paired *t*-test vs A_0 in the presence of $BaCl_2$. **C** PE-sensitive difference A_0 currents in control cells (*n*=44), in the presence of 1mM $ZnCl_2$ (*n*=9) and 10mM $BaCl_2$ (*n*=8). †††: p<0.001, unpaired *t*-test vs control.

Figure 7. Effect of external 4-aminopyridine on the PE-sensitive current. **A** Concentration dependence of the effect of 4-aminopyridine on the time-independent (A_0) current. Numbers in brackets represent cell numbers. Solid line represents a fit to a logistic equation with a Hill

Molecular Pharmacology Fast Forward. Published on June 24, 2004 as DOI: 10.1124/mol.104.000760
This article has not been copyedited and formatted. The final version may differ from this version.

coefficient of 2 (equation 6). The maximal current inhibition was 20.7% and the IC_{50} was 0.68μM. Dotted line represents fit to a logistic equation with a Hill coefficient of 1. **B** Example current traces under control conditions, in the presence of 10mM 4-aminopyridine (4-AP) and in the presence of 10mM 4-AP plus 10μM PE. Solid lines represent fits to a double exponential relation (equation 4). **C** Mean ± S.E.M of PE-sensitive A_0 difference currents under control conditions (*n*=44) and in the presence of 10mM 4-AP (*n*=8). ***: p<0.001, unpaired *t*-test vs control PE-sensitive A_0 difference current. The PE-sensitive current was also significantly reduced in the presence of 3mM 4-AP (1.04 ± 0.37 pA/pF; *n*=6). The effect of 3mM 4-AP was not significantly different from 10mM 4-AP (unpaired *t*-test).

Figure 8. Effect of external TEA on PE-sensitive current. **A** Upper panel shows example current traces under control conditions, in the presence of 10mM external TEA (TEA_e) and in the presence of 10mM TEA_e plus 10μM PE. Solid lines represent fits to a double exponential relation (equation 4). Lower panel shows the mean ± S.E.M of the time-independent (A_0) and inactivating (A_1+A_2) currents for 6 cells exposed to 10mM TEA_e. *: p<0.05, paired *t*-test compared to control. **: p<0.01, paired *t*-test compared to A_0 in the presence of TEA_e. †: p<0.05, paired *t*-test vs A_1+A_2 current in the presence of 10mM TEA_e. **B** Upper panel shows example current traces in the presence of 50mM TEA_e and 50mM TEA_e plus 10μM PE. Solid lines represent fits to a double exponential equation. Lower panel shows the mean ± S.E.M of the time-independent (A_0) and inactivating (A_1+A_2) currents for 6 cells exposed to 50mM TEA_e. †††: p<0.001, unpaired *t*-test vs corresponding control current densities. **: p<0.01, paired *t*-test vs A_0 in the presence of 50mM TEA_e. *: p<0.05, paired *t*-test vs A_1+A_2 current in the presence of 50mM TEA_e. **C** Mean ± S.E.M of PE-sensitive A_0 difference currents under control conditions (C, *n*=44) and in the presence of 10mM (*n*=6) and 50mM (*n*=6) TEA_e. ††:

p<0.01, unpaired *t*-test vs control PE-sensitive A_0 difference current. †††: p<0.001, unpaired *t*-test vs control PE-sensitive A_0 difference current.

Figure 9. Spectral analysis of PE-sensitive current. **A** Example current traces under control conditions (gray) and in the presence of 10μM PE (black). Inset shows the last 1024 data points of the current traces after subtraction of the DC and inactivating components. **B** Power spectra of the control current (open triangles) and the current in the presence of PE (open squares) for the data shown in A. Filled circles represents the power spectrum of the PE-sensitive component calculated by subtracting the background power spectrum from control. Solid line represents a fit to the PE-sensitive power spectrum using equation 8 (S(0) = 26.4pA^{2}s, f_c = 124Hz). The single channel conductance calculated using equation 10, γ = 75.2pS.

Figure 10. Effect of quinidine on the PE-sensitive current. **A** Upper panel shows example current traces under control conditions, in the presence of 100μM external quinidine (Qui) and in the presence of 100μM Qui plus 10μM PE. Solid lines represent fits to a double exponential relation (equation 4). **B** Left-hand panel shows the mean ± S.E.M of the time-independent (A_0) and the right-hand panel shows the inactivating (A_1+A_2) currents for 6 cells exposed to 100μM Qui. *: p<0.05, paired *t*-test compared to A_0 in the presence of 100μM Qui. **: p<0.01, paired *t*-test compared to control. **C** Mean ± S.E.M of PE-sensitive A_0 difference currents under control conditions (C, *n*=44) and in the presence of 100μM Qui (*n*=6). †††: p<0.001, unpaired *t*-test vs control PE-sensitive A_0 difference current.

Figure 11. The response to PE is mediated predominantly by α_{1A}-adrenoceptors. **A** Mean ± S.E.M of PE-sensitive current amplitudes under control conditions (*n*=44), in the presence of 1μM prazosin (*n*=7), after pretreatment with 30μM chloroethylclonidine (CEC, *n*=5) and 100nM WB4101 (*n*=6) and the A61603-sensitive difference current (*n*=8). ††: p<0.01,

unpaired *t*-test with control. †††: p<0.001, unpaired *t*-test with control. Control A_0 was not significantly affected by either 1μM prazosin or 100nM WB4101. The response to 10μM PE was not significantly reduced by a lower concentration (1nM) of the competitive antagonist, prazosin (1.62 ± 0.45 pA/pF, *n*=5). **B** Upper panel shows example current traces from a cell pre-treated with 30μM CEC before and after superfusion with 10μM PE. Solid lines represent fits to a double exponential equation. Lower panel shows PE-sensitive difference current. **C** Upper panel shows example current traces before and after superfusion with 100nM A61603. Solid lines represent fits to a double exponential equation. Lower panel shows A61603-sensitive difference current.

Figure 12. The response to PE is mediated by a Ca^{2+}-independent pathway involving a PTX-insensitive G-protein and PI 3-kinase. **A** Mean ± S.E.M of PE-sensitive current from control cells (*n*=44), from cells dialyzed with a pipette solution containing 1mM GDPβS (*n*=7), from cells pre-treated with 7.5μg/ml PTX (*n*=5), from cells dialyzed with a pipette solution containing 10μM GP2A (*n*=5) and from cells dialyzed with a nominally Ca^{2+}-free pipette solution containing 10mM BAPTA (*n*=7). ††: p<0.01, unpaired *t*-test vs control. †††: p<0.001, unpaired *t*-test vs control. **B** Mean ± S.E.M of PE-sensitive current from cells treated with phospholipase inhibitors. Cells were pre-treated with 5μM U73122 (*n*=5), 5μM U73343 (*n*=11), 2mM neomycin sulfate (*n*=5), 40μM $AACOCF_3$ (*n*=8) or 25μM MAFP (*n*=4). ††: p<0.01, unpaired *t*-test vs control. †††: p<0.001, unpaired *t*-test vs control. **C** Mean ± S.E.M of PE-sensitive current in cells treated with various kinase inhibitors. The PKCε-specific peptide antagonist (αPKCε; 75μM, *n*=3) and wortmannin (5μM, *n*=5) were applied via the pipette solution. Cells were pre-treated for 30 min with 200nM staurosporine (*n*=4), 1μM GF109203X (*n*=5) and 50μM genistein (*n*=7). †: p<0.05, unpaired *t*-test vs control. ††: p<0.01, unpaired *t*-test vs control. GDPβS, GP2A, U73122, $AACOCF_3$ and wortmannin had

Molecular Pharmacology Fast Forward. Published on June 24, 2004 as DOI: 10.1124/mol.104.000760
This article has not been copyedited and formatted. The final version may differ from this version.

no significant effect on the control current. However, the control current was significantly inhibited by genistein (from 4.83 ± 0.36 pA/pF to 3.22 ± 0.40 pA/pF, $p<0.001$, $n=7$).

Molecular Pharmacology Fast Forward. Published on June 24, 2004 as DOI: 10.1124/mol.104.000760
This article has not been copyedited and formatted. The final version may differ from this version.

TABLES

Table 1. Mean (± S.E.M.) of fitted parameters from 7 cells of voltage-dependent inactivation according to a single Boltzmann equation.

Parameter	Control	10μM PE	P
$\mathbf{I_t}$	11.11 ± 2.50 pA/pF	9.04 ± 1.31 pA/pF	ns
$\mathbf{V_{0.5}}$	-45.9 ± 3.1 mV	-43.4 ± 0.31 mV	ns
$\mathbf{V_s}$	7.5 ± 0.8 mV	9.6 ± 0.9 mV	ns
$\mathbf{I_{ss}}$	6.10 ± 0.50 pA/pF	4.45 ± 0.31 pA/pF	P < 0.02

Molecular Pharmacology Fast Forward. Published on June 24, 2004 as DOI: 10.1124/mol.104.000760
This article has not been copyedited and formatted. The final version may differ from this version.

Figure 1

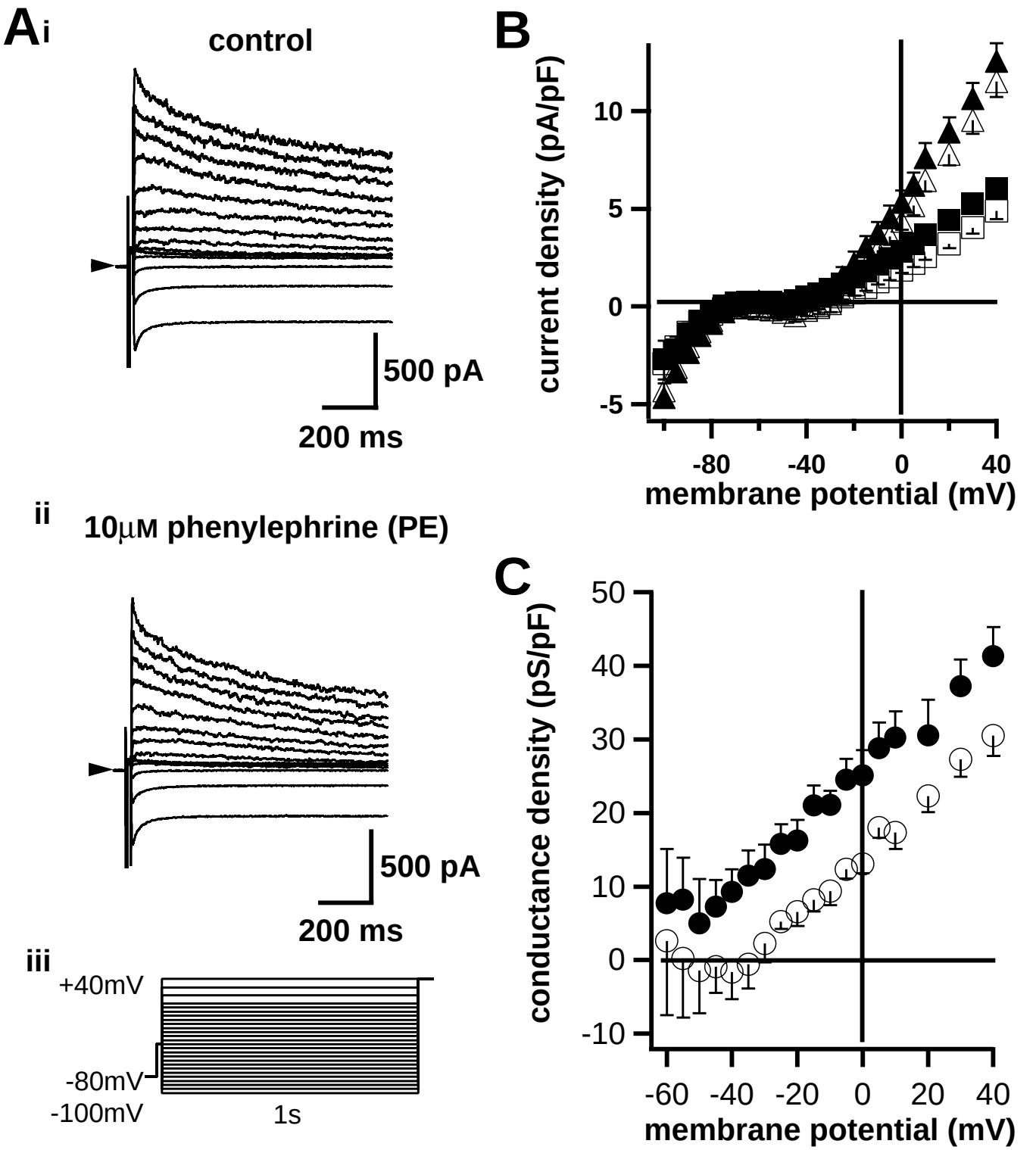

Figure 2

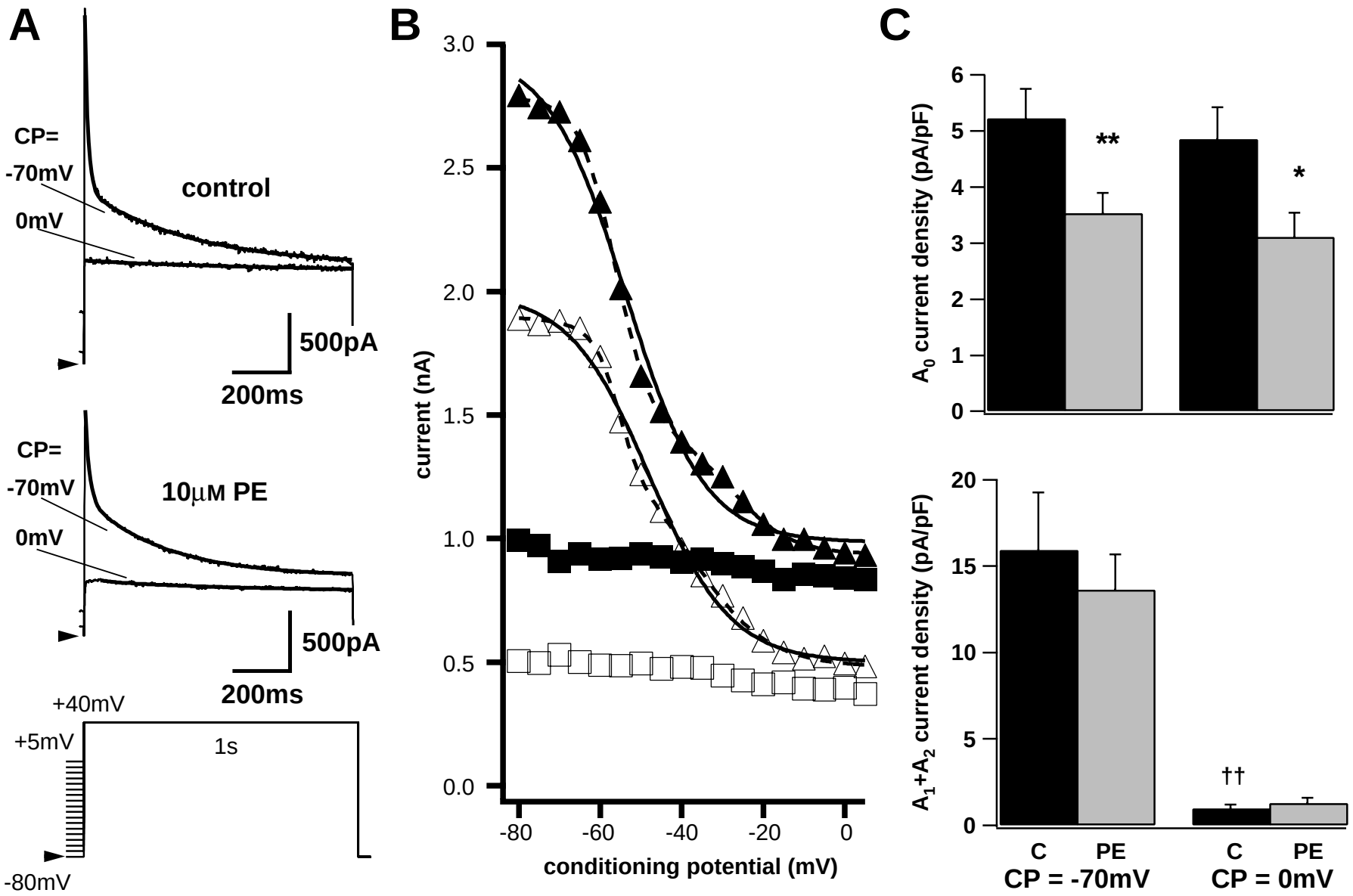

Molecular Pharmacology Fast Forward. Published on June 24, 2004 as DOI: 10.1124/mol.104.000760
This article has not been copyedited and formatted. The final version may differ from this version.

Figure 3

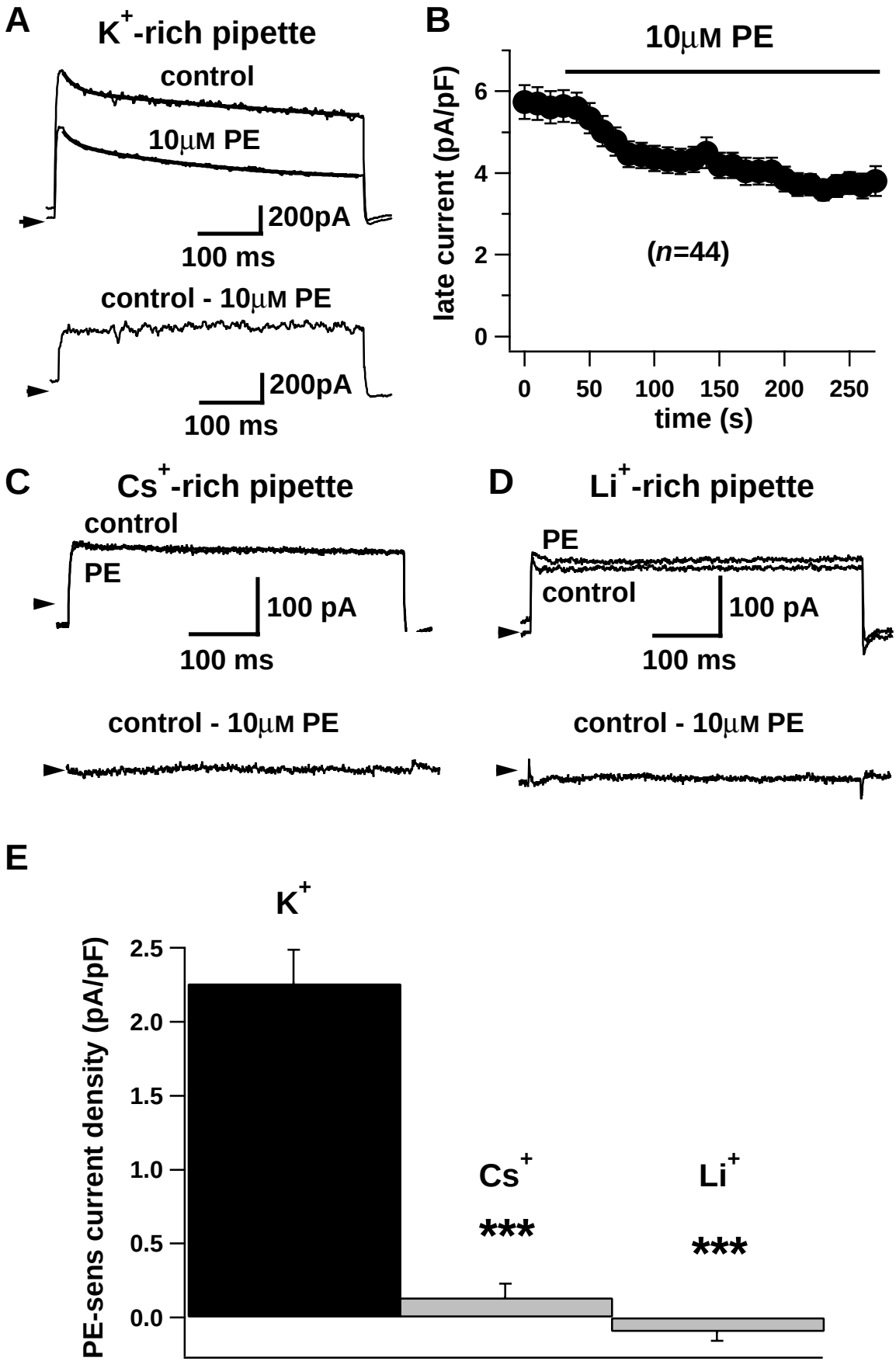

Molecular Pharmacology Fast Forward. Published on June 24, 2004 as DOI: 10.1124/mol.104.000760
This article has not been copyedited and formatted. The final version may differ from this version.

Figure 4

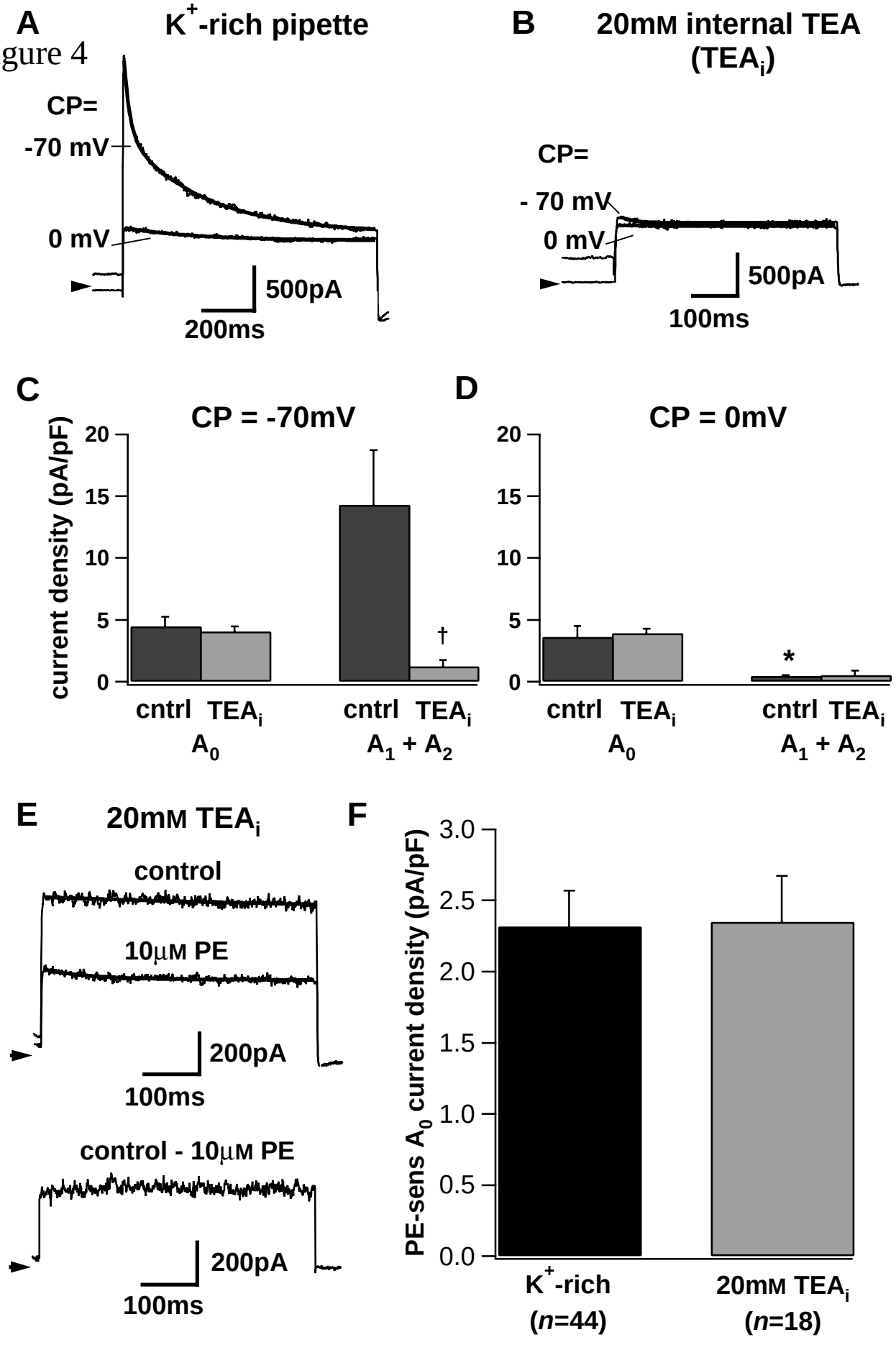

Molecular Pharmacology Fast Forward. Published on June 24, 2004 as DOI: 10.1124/mol.104.000760
This article has not been copyedited and formatted. The final version may differ from this version.

Figure 5

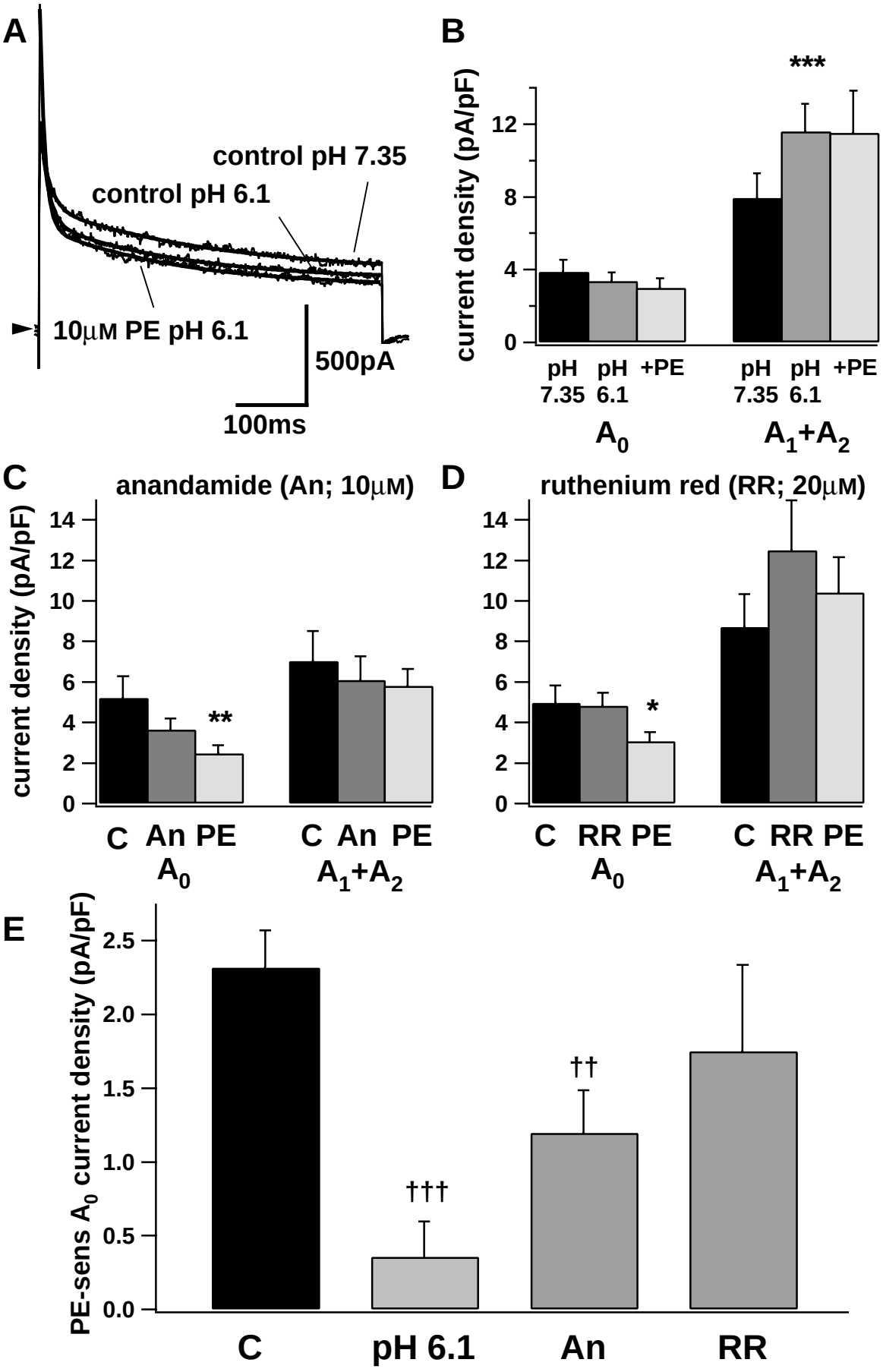

Molecular Pharmacology Fast Forward. Published on June 24, 2004 as DOI: 10.1124/mol.104.000760
This article has not been copyedited and formatted. The final version may differ from this version.

Figure 6

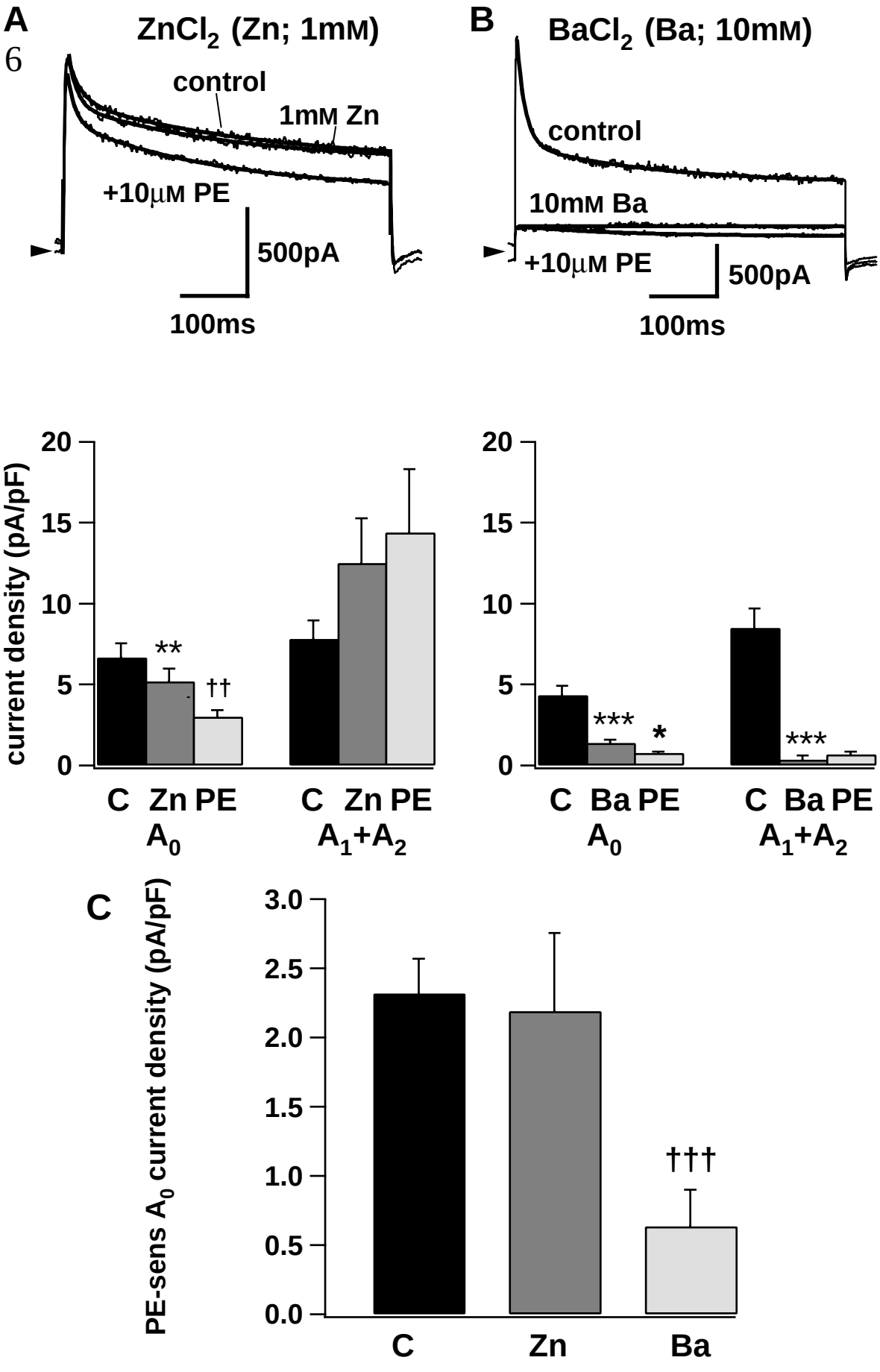

Figure 7

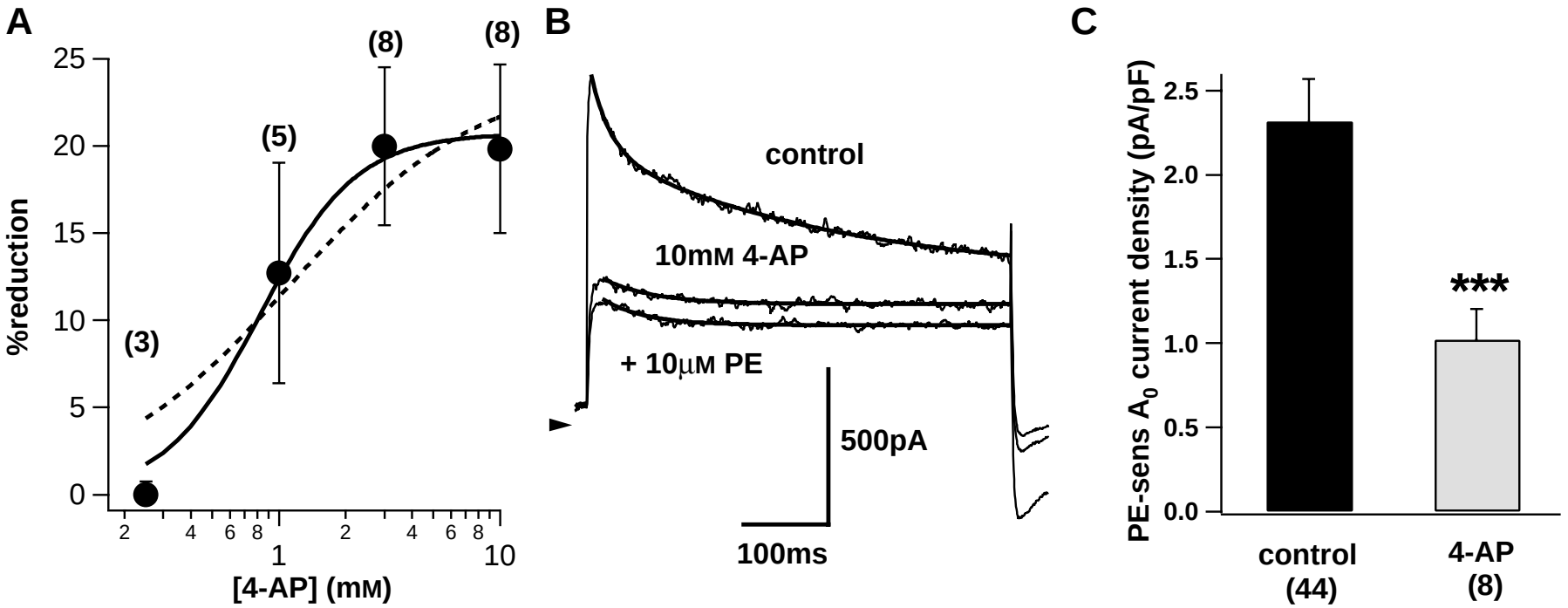

Molecular Pharmacology Fast Forward. Published on June 24, 2004 as DOI: 10.1124/mol.104.000760
This article has not been copyedited and formatted. The final version may differ from this version.

Figure 8

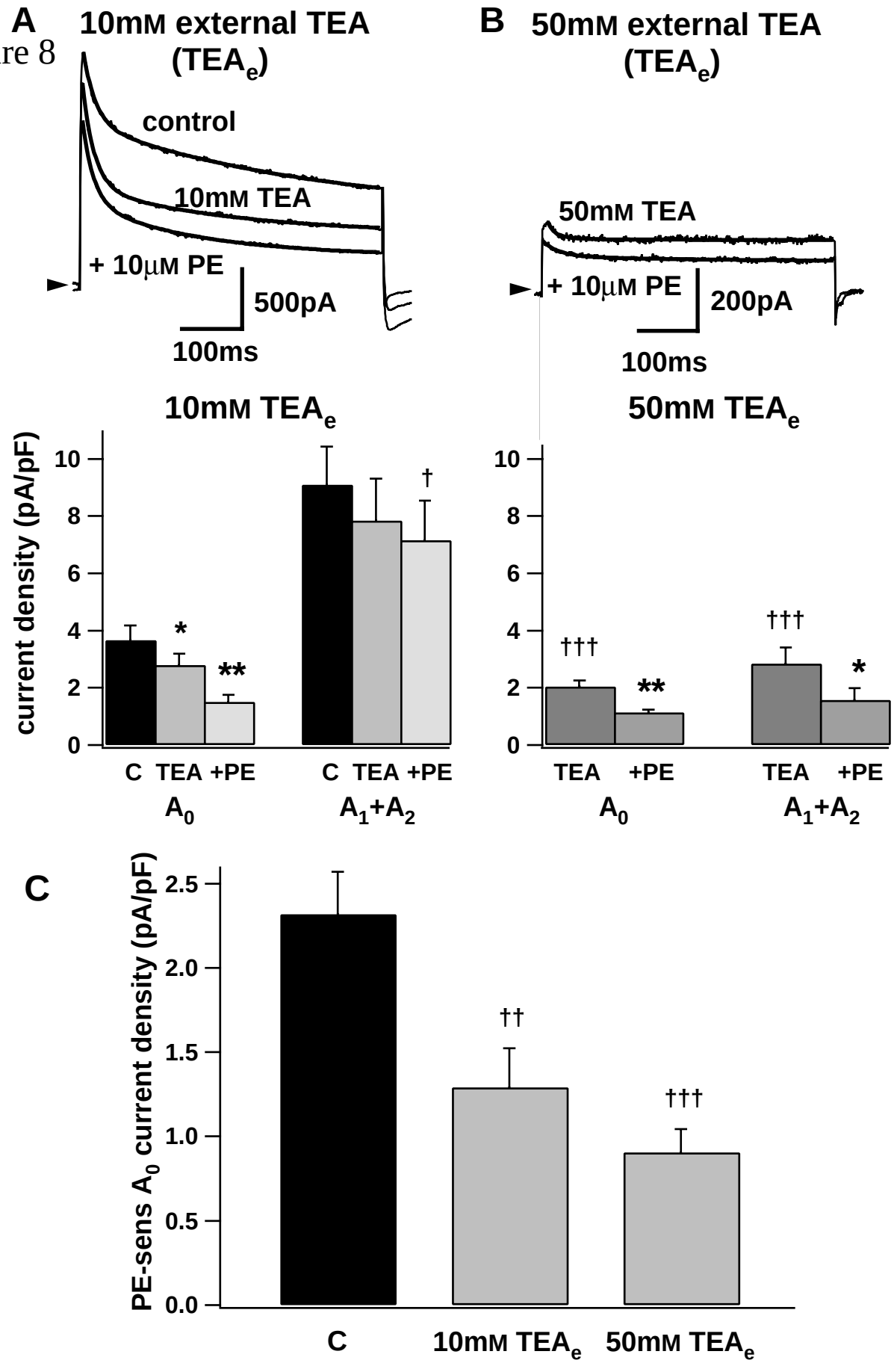

Molecular Pharmacology Fast Forward. Published on June 24, 2004 as DOI: 10.1124/mol.104.000760
This article has not been copyedited and formatted. The final version may differ from this version.

Figure 9

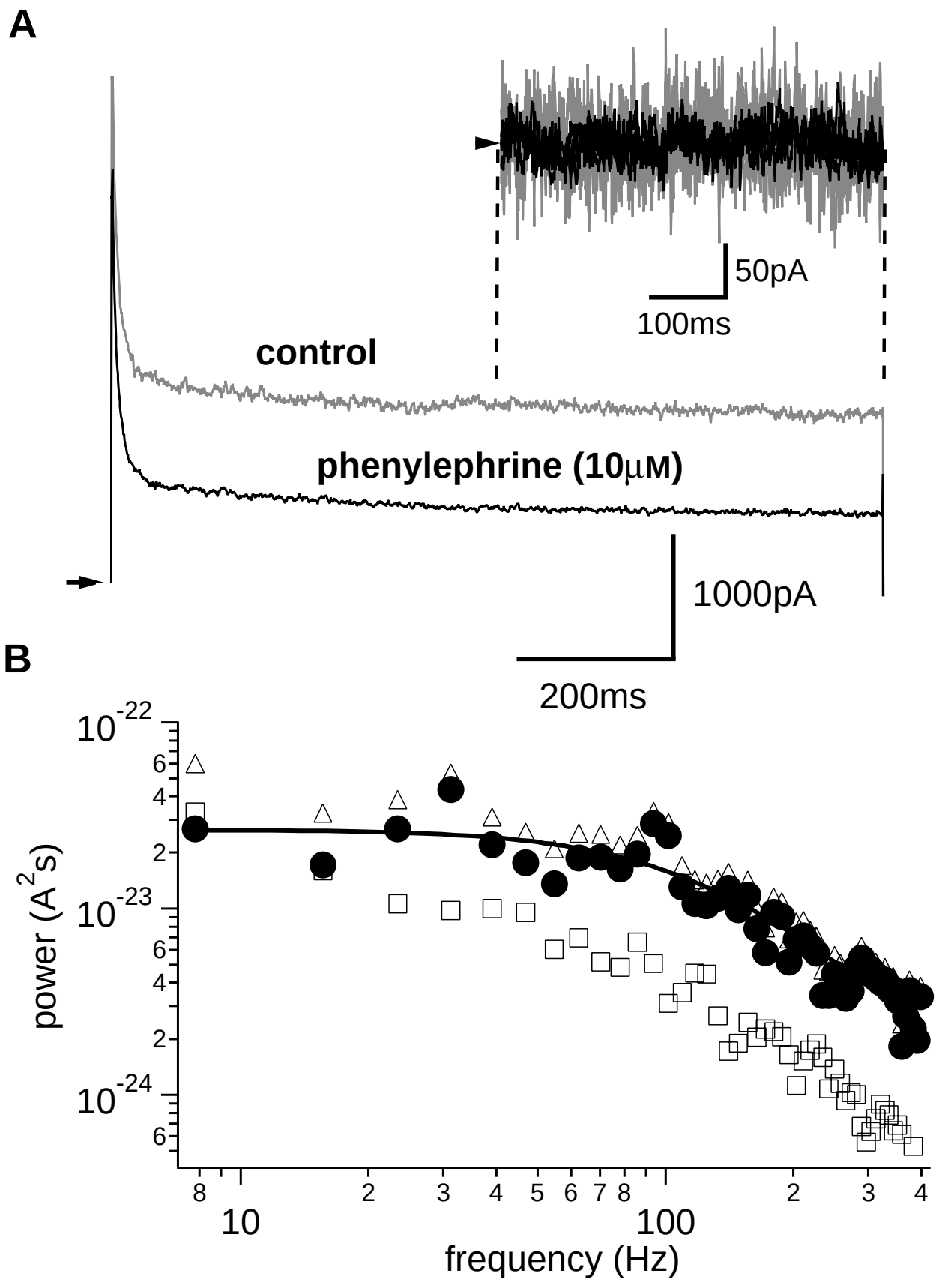

Molecular Pharmacology Fast Forward. Published on June 24, 2004 as DOI: 10.1124/mol.104.000760
This article has not been copyedited and formatted. The final version may differ from this version.

Figure 10

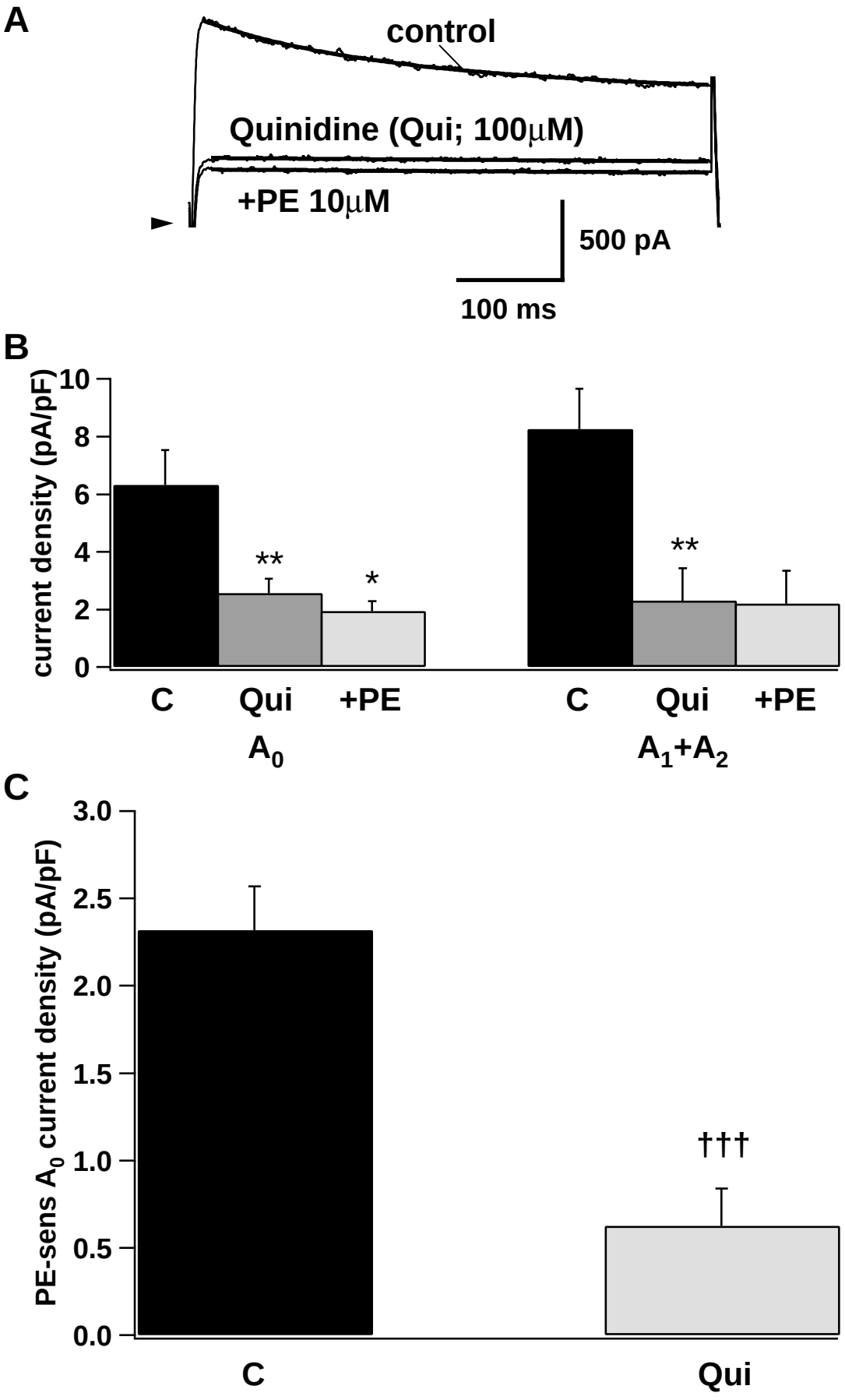

Figure 11

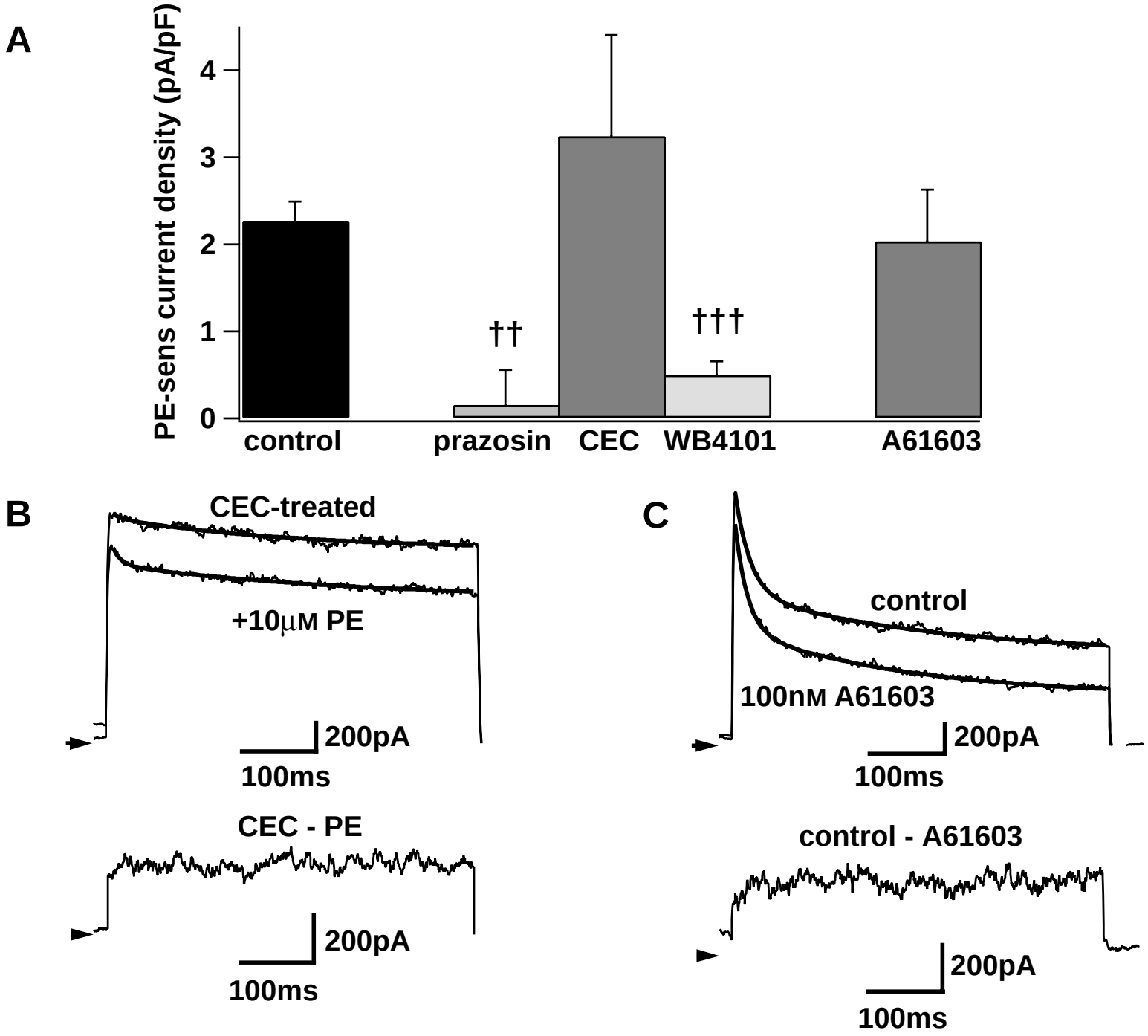

Molecular Pharmacology Fast Forward. Published on June 24, 2004 as DOI: 10.1124/mol.104.000760
This article has not been copyedited and formatted. The final version may differ from this version.

Figure 12